M 2018

U. PORTO

FEUP FACULDADE DE ENGENHARIA
UNIVERSIDADE DO PORTO

COATING FORMULATIONS BASED ON HIGH PERFORMANCE POLYMERS FOR LOW-FRICTION AND LOW-WEAR APPLICATIONS

FILIPA GUEDES
DISSERTAÇÃO DE MESTRADO APRESENTADA
À FACULDADE DE ENGENHARIA DA UNIVERSIDADE DO PORTO EM
ENGENHARIA QUÍMICA

Master in Chemical Engineering

Coating formulations based on high performance polymers for low-friction and low-wear applications

A Master's dissertation

of

Filipa Guedes

Developed within the course of dissertation

held in

Tribochem, Lda.

Supervisor at FEUP: **Professor Fernão de Magalhães**

Supervisor at Tribochem: **Engineer Judith M. Pedroso**

U.PORTO

FEUP **FACULDADE DE ENGENHARIA**
UNIVERSIDADE DO PORTO

Departamento de Engenharia Química

July of 2018

Acknowledgment

The work developed during the last months would not be possible without the contribution of several people to whom I would like to thank.

To my supervisor at FEUP, Professor Fernão de Magalhães, for supervising my work and for the constant availability.

To my supervisor at Tribochem, Engineer Judith M. Pedroso, for all the knowledge and experience shared, which were crucial for the success of this project and to my self-development, for all the comprehension and constant availability.

To Tribochem and its team, for allowing me to be part of this project and for supporting me during all the work.

To Professor Margarida Bastos, for the time spent helping me with some analysis.

To my parents, for allowing me the opportunity to be where I am, for all the patience, for inspiring me and being an example.

To my dinosaur, for all the patience, for supporting me specially in the most complicated days and for not give up on make me laugh.

To my friends, the true ones, for all the supporting and for the sharing of all the moments that contributed to make me a better person.

To my dragons, for make me fly with them.

As it could not be forgotten, I am thankful for being a turtle born in the middle of a killer whales' army in Olimpo.

Abstract

Today, with the development of technology, it comes the necessity of products with excellent performance to reduce the costs of maintenance. Therefore, it came the opportunity to develop a coating with a liquid crystal polymer that has interesting properties such as its high thermal stability. The main objective of this work is develop a formulation of a coating that presents low friction and low wear in order to prevent costs and to increase the lifetime of the product.

During the present work, in a first instance, it was made a physico-chemical characterization of the several liquid crystal polymers and then it was tested the solubilization. After, a coating formulation was achieved and applied. In the last part of this project, it was made a mechanical and tribological characterization of the coating.

From four different grades of LCP, the solubilization was possible for two grades of them. To help the processing in the laboratory, the one that is presented in the pellet form was selected to perform the formulation. A stable formulation was achieved and then the mechanical and tribological characterization of the coating was performed, after the application and curing process of the formulation.

At the end, it was achieved a high performance coating that presents a low coefficient of friction, as it was intended. Regarding wear, the results were inconclusive since the conditions of tribological test used were too low. The coating was compared with a commercial one and the performance of both seems to be similar in terms of friction.

Keywords: Liquid Crystal Polymer; Coating; Tribology; Friction; Wear.

Resumo

Hoje em dia, com o desenvolvimento da tecnologia, surge a necessidade de produtos com elevado desempenho para reduzir os custos de manutenção. Assim, surgiu a oportunidade de desenvolver um revestimento com polímeros de cristais líquidos, que apresentam propriedades interessantes como, por exemplo, a sua elevada estabilidade térmica. O principal objetivo deste trabalho é obter uma formulação de um revestimento que apresente baixo atrito e baixo desgaste, de modo a evitar custos e a aumentar o tempo de vida do produto.

Durante o presente trabalho, numa fase inicial, foi realizada uma caracterização físico-química de vários polímeros de cristais líquidos e foi testada a sua solubilização. De seguida, foi conseguida uma formulação do revestimento que foi possível aplicar. Na última parte do projeto, foi feita uma caracterização mecânica e tribológica do revestimento.

Entre quatro diferentes amostras de LCP, apenas foi possível a solubilização de dois deles. Para facilitar o processamento em ambiente laboratorial, foi escolhida uma das amostras de LCP solúvel, que se encontra sob a forma de pastilha. Foi possível desenvolver uma formulação estável, tendo sido de seguida realizada a caracterização mecânica e tribológica do revestimento após a aplicação e processo de cura da formulação.

Por fim, foi conseguido um revestimento de elevado desempenho que apresenta baixo coeficiente de atrito, como se pretendia. Relativamente ao desgaste, os resultados foram inconclusivos uma vez que as condições utilizadas nos testes tribológicos foram demasiado baixas. O revestimento foi comparado com um revestimento comercial e o desempenho de ambos aparenta ser semelhante em termos de coeficiente de atrito.

Palavras chave: Polímeros de Cristais Líquidos; Revestimento; Tribologia; Atrito; Desgaste.

Declaration

I hereby declare, on my word of honor, that this work is original and that all non-original contributions were properly referenced with source identification.

02 / 07 / 2018   _Filipa Guedes_

                                                                                    (Filipa Guedes)

Index

Notation and Glossary

cps	Counts per second	
d	Sliding distance	m
L	Load	N
p	Average pressure (carrying load per unit length)	N·m^{-1}
R_a	Roughness average	μm
T_c	Clearing temperature	°C
T_{C-LC}	*Crystalline-liquid crystalline transition temperature*	°C
T_g	Glass transition temperature	°C
T_m	Melting temperature	°C
U	Sliding velocity	m·s^{-1}
V_r	Removed volume	mm^3
$\dot{W}$	Wear rate	mm^3·N^{-1}·m^{-1}

Greek Letters

η	Lubricant viscosity	N·s·m^{-2}
θ	Incidence angle	°
λ	Wavelength	Å

List of Acronyms

ATR	Attenuated total reflection
BSD	Backscattered electron detector
DSC	Differential scanning calorimetry
EDS	Energy Dispersive X-Ray Spectroscopy
FTIR	Fourier-transform infrared
IFIMUP	Instituto de Física dos Materiais da Universidade do Porto
LC	Liquid Crystal
LCP	Liquid Crystal Polymer
NMP	N-methyl-2-pyrolidone
PAI	Polyamide-imide
PTFE	Polytetrafluorethylene
SED	Secondary electrons detector
SEM	Scanning Electron Microscopy
TGA	Thermogravimetric analysis
XRD	X-Ray diffraction

1 Introduction

1.1 Framing and presentation of the work

Nowadays, with the advance of technology, the consumers are much more exigent and give importance to the little aspects that promote the reduction of the cost as well as the good performance of the product. Such as, it came the opportunity to develop a coating with low friction and low wear, which can reduce the maintenance costs. Besides that, it is a product that does not exist in the market, which makes it more attractive, and the polymer used has unique properties such as its high thermal stability. The main goal of the present work is obtain a stable formulation of the coating that allows a low coefficient of friction and low wear.

1.2 Presentation of the company

Tribochem is a startup company that consists in a team formed by Flupol, Surface Engineering and a multinational company. The main objective of Tribochem is create and improve formulations, based on polymeric coatings or other matrices with commercial interest, in order to have improved mechanical characteristics. Flupol gives support in the application of the formulations and the multinational company assists the mechanical characterization.

1.3 Contributions of the Work

The achievement of a formulation that is stable and adhere to the substrate is for itself a big step for Tribochem since before this work it was reached a formulation that did not stabilize. To complement that, it was possible to obtain a low coefficient of friction, which was the main objective. This work allowed the knowledge of the limitations to solubilize the polymer and to keep the formulation stable, which is useful for Tribochem to can continue to improve it.

1.4 Organization of the thesis

This thesis is organized in six main chapters: Introduction, State of the art, Materials and methods, Results and discussion, Conclusions and Assessments of the work done.

The Introduction chapter frames the thesis work and presents the company.

In the second chapter, the State of the Art, there are introduced all the theoretically concepts that allow the understanding of the developed work.

The Materials and methods chapter presents all the materials and equipment used as well as some characteristics of them.

The Results and discussion chapter presents the achieved results and the decisions made as well as some bibliographic support that was used to corroborate the results obtained.

The Conclusions chapter contains the conclusions obtained by the analysis of the previously chapter.

The final chapter, Assessments of the work done, contains an evaluation of the work done as well as the limitations found during the project and suggestions for a future work.

2 Context and State of the art

2.1 Liquid Crystal Polymers

2.1.1 History

Liquid Crystals (LCs) were discovered by the botanist Friedrich Reinitzer, in 1888 through the observation of the cholesteryl esters that, when melted, formed opaque liquids which became clear with the raise of temperature. Taking this situation into account, Reinitzer decided to send a sample to the physicist Otto Lemann, who has concluded that it was a new state of matter, naming it as *liquid crystal* in 1900 (Pavel et al. 2006; Shibaev 2016). Figure 1 shows the first LC studied.
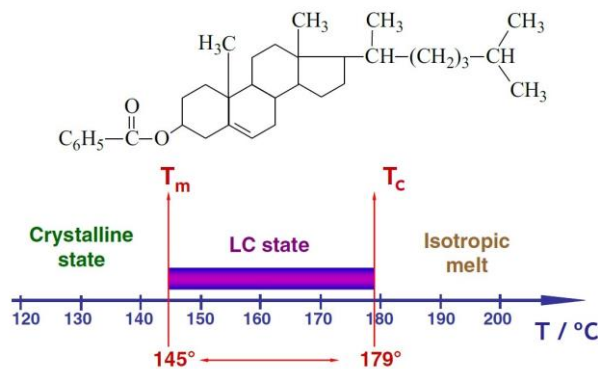

Figure 1 - Cholesteryl benzoate structure and respetively temperature range LC phase diagram (Shibaev 2016).

2.1.2 Liquid Crystals

The degree of macroscopic orientational order of Liquid Crystals (LCs) is an intermediate between the crystalline solid and the liquid isotropic states, so the LCs' properties are too intermediate between the two states. LCs are anisotropic materials, which means that the properties depend on the direction in which they are measured, so their flow properties are dependent of their structure and molecular orientation (Pavel et al. 2006).

When a crystalline solid material is heated, it melts into an isotropic liquid and loses the orientational and positional order, being the temperature at which it happens called *melting temperature, T_m*. When the isotropic liquid is then cooled, it solidifies again. However, there are materials that have a different behavior since they do not show a single transition between the two states. Such materials exhibit an intermediate phase, called liquid crystalline phase or mesophase. These materials only loose its ordering partially, and the melting point coincides with the *crystalline-liquid crystalline transition temperature, T_{C-LC}*. The mesophase, when exposed at higher temperatures, loses its partial order and goes through a liquid

crystalline-isotropic transition, being transformed into an isotropic liquid at a *clearing temperature*, T_c. The temperature range between T_m and T_c represents the thermodynamically stability of the liquid crystalline phase (Pavel et al. 2006).

According to the conditions of liquid crystalline phase formation, liquid crystals can be thermotropic, if this phase is formed by heating a solid, or lyotropic if there is dissolution of the solid in a solvent (Shibaev 2016). Figure 2 shows the transition temperature of thermotropic LCs.
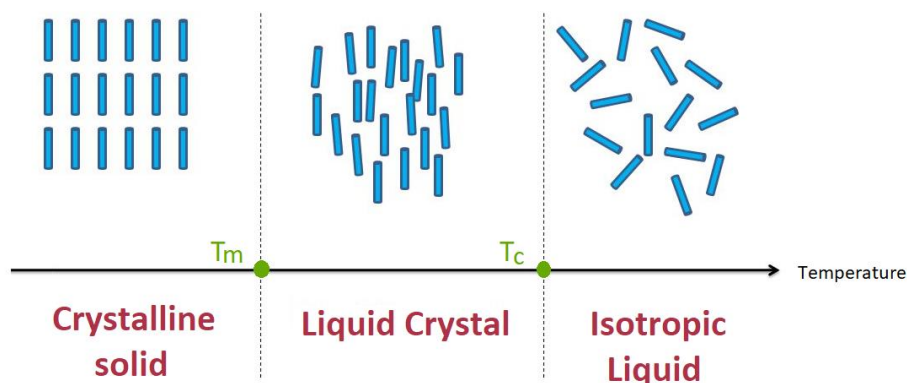

Figure 2 - Thermotropic liquid crystalline transition. Adapted from ("Wayne State University" 2008).

Lyotropic liquid crystals are formed by two or more components which have LC properties in a certain concentration range in a solution. There is formation of molecular aggregates or micelles due to the interactions between the amphiphilic and the solvent molecules. The amphiphilic molecules are a constituent of the LC, composed by two parts - a hydrophilic and a hydrophobic one. The function of the solvent molecules is to fill the space around the LC compounds in order to provide fluidity to the system (Shibaev 2016). Figure 3 shows the concentration transition of lyotropic LCs.
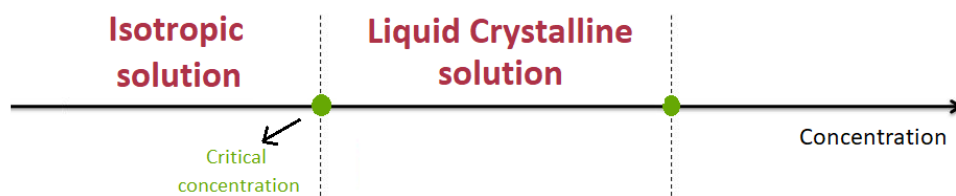

Figure 3 - Lyotropic liquid crystalline transition. Adapted from (Pavel et al. 2006).

2.1.3   Liquid Crystal Polymers

Liquid Crystal Polymers (LCPs) are constituted by mesogenic units that often consist of rigid core of two or more aromatic rings and are linked by flexible spacers. The mesogenic

group increases the anisotropic interactions between the molecules, raising the clearing temperature. The flexible spacers are responsible for a high number of conformations of the molecules and so for the increase of the entropy of melting, reducing the melting temperature. Figure 4 shows some examples of mesogenic units of LCPs (Pavel et al. 2006).
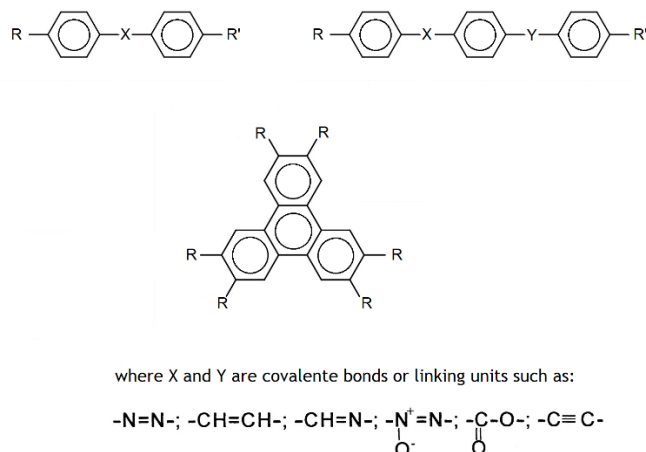
where X and Y are covalente bonds or linking units such as:

$-N=N-; -CH=CH-; -CH=N-; -N^+=N-; -C-O-; -C\equiv C-$

Figure 4 - Examples of mesogenic groups (Báron 2001).

Regarding the position of the mesogenic groups, liquid crystal polymers are classified as *main-chain, side-chain, cross-linked* and a combination of the main-chain and side-chain. The *main-chain* LCP is characterized by the mesogenic groups being incorporated in the backbone of the polymer. If the mesogenic groups are attached onto the polymer as side-chains, through a flexible spacer or directly, LCP is called *side-chain*. *Cross-linked* LCP, also known as network or thermoset, are formed by a cross-linking reaction of LCPs that are functionalized with reactive groups. The last type, *combined main-chain/side-chain*, is formed when the mesogenic groups are incorporated into and onto the polymer main-chain, through a flexible spacer or directly. These four types of polymers are schematically represented in Figure 5, where the cylindrical unit represents the mesogen (Pavel et al. 2006; Shibaev 2016).

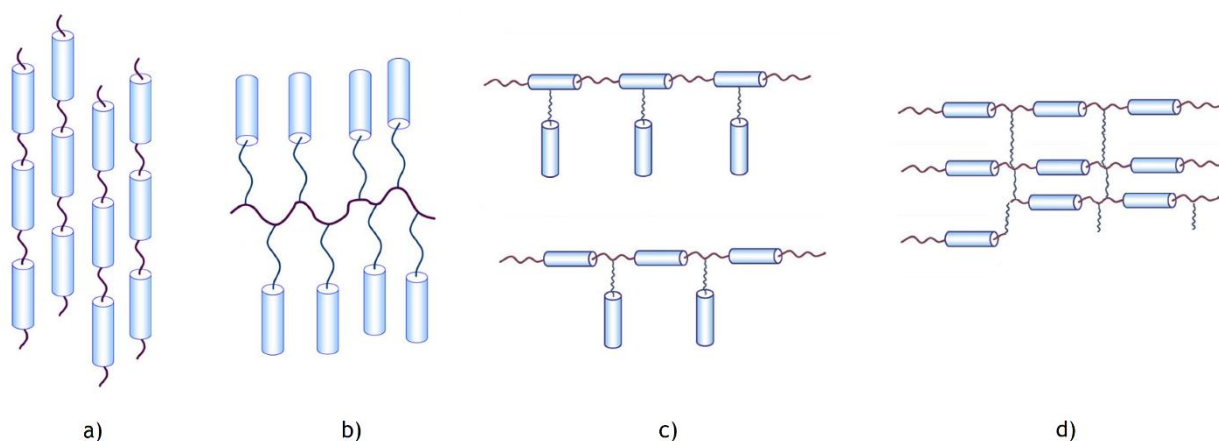a)   b)   c)   d)

Figure 5 - Schematic representation of the polymer chain: a) main-chain; b) side-chain;
c) combined main-chain/side-chain, d) cross-linked. Adapted from (Pavel et al. 2006).

The requirement for the formation of a liquid crystalline phase is the anisotropy, which means that one of the molecular dimensions has to be larger or smaller than the others. Thus, the mesogenic group has a rod-like or a disc-like nature (Pavel et al. 2006). Most of the rod-shaped LCP have one to three benzene rings linked directly or via linking units as –CH=CH-, -CH=N-, -NH-CO-, -COO-, while disk-shaped LC are constituted by a rigid central part and four to eight flexible chains attached to the core (Shibaev 2016).

2.1.4 Properties and Applications

LCP is a material with unique physical properties, presenting a high glass transition temperature (T_g) and high melting point, hence conferring it a high thermal stability (Shibaev 2016). Besides this, LCP has low water absorbency that prevent changes caused by humidity and low gas emission that confers protection from corrosion. LCP is recyclable, has low flammability and presents good electrical properties (Miyauchi et al. 2016; Cosimo et al. 1999; Xuefeng et al. 2003). Table 1 presents some properties of LCPs and their area of application.

Table 1 - Areas of application of LCP and important properties related to them (Pavel et al. 2006; Cosimo et al. 1999).

Application Area	Properties of main interest	Application
Electronics	- Thermal conductivity - Low dielectric constant - Resistance to corrosive compounds	Connectors, optical amplifiers, antennas, electronic package, switches
Optical Fiber	- Low flammability - Good mechanical properties	Couplers, connectors
Medicine	- Non-toxicity - Low permeability - Compatibility with the sterilization techniques	Pharmacological tests, optical filters and membranes, cancer diagnosis
Automotive	- Excellent mechanical, chemical and electrical properties - Toughness - Resistance to solvents - Thermal resistance	Fuel system components, automobile parts, electronic compounds
Domestic	- Thermal and chemical resistance - Toughness	Microwave components, pump housing

One of the most known LCP is poly-p-phenyleneterephthalamide , also known as Kevlar® (Wang and Zhou 2004). This polymer is popular due its application on bulletproof vests and its structure is presented in Figure 6.
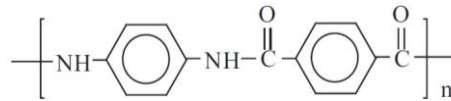

Figure 6 – Chemical structure of Kevlar® (Wang and Zhou 2004).

2.2 Tribology

The term tribology is derived from the Greek word *tribos*, which means rubbing (Carrión et al. 2009). This science is related to contact mechanisms of interaction between surfaces in relative motion, which normally involves energy dissipation. The tribological characterization of materials deals with parameters such as friction, wear and lubrication, which may be studied in order to minimize and eliminate the energy dissipation and to provide better performance and efficiency (Brostow et al. 2003; Bhushan 2013b).

The tribological system is constituted by four elements: the two contacting materials, the interface between the contact pair, the medium in the interface and the environment (Theo 2011). Figure 7 shows an example of a tribological system.
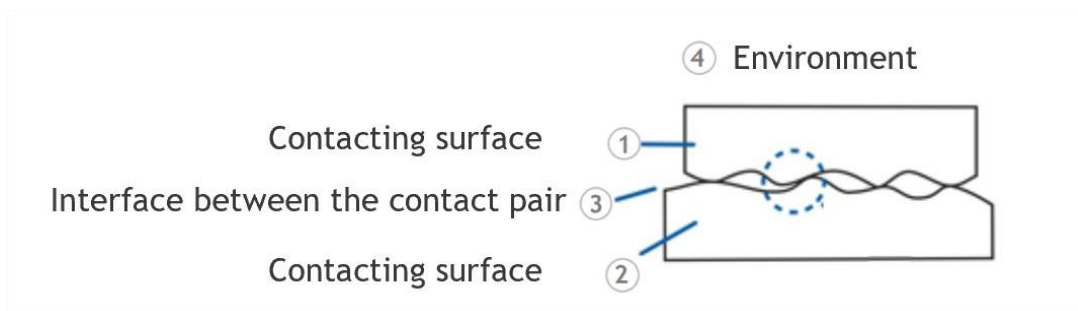

Figure 7 - Elements of a tribological system. Adapted from ("GGB").

2.2.1 History

The word *tribology* was coined in 1966 in a report of the United Kingdom Department of Education and Science, being a concept introduced by Peter Josh (Myshkin and Goryacheva 2016). However, tribology was already applied in the Stone Age. During the Paleolithic period, the friction between pieces of stones was used to produce fire and bearings made of bones and antlers were used for drilling holes (Bhushan 2013c).

The use of wheels, dated from 3500 B.C., shows one of the approaches in order to reduce the friction during displacement movements. The meaning of the concept lubricant was born after the Egyptians verified the difficulty to transport big stones and monuments. In Figure 8 it is possible to see a sledge used for transportation of a heavy statue, by the Egyptians, circa 1880 B.C (Bhushan 2013c).
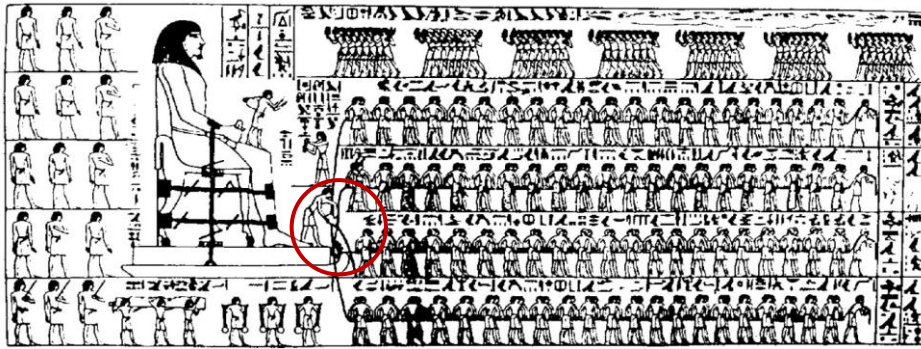
Figure 8 - Egyptians using lubricant to help the transportation of a statue (Bhushan 2013b).

In the transportation were involved 172 slaves that dragged a statue weighing about 660 kN along a wooden track and the man standing on the sledge was putting a liquid into the path of motion, which probably worked as a lubricant to help the transportation. Besides this, a chariot, dated thousand years B.C., was found in a tomb in Egypt and it contained lubricants of animal-fat in its wheels bearings (Bhushan 2013b).

During and after the Romane Empire, military engineers created war machines using tribological principles (Bhushan 2013b). Leonardo Da Vinci (1452-1519) was aware of the concepts of friction, lubrication and wear. Although his discoveries and developments in these fields remained unknown for tribologists until 20th century, and so he had no influence on the development of the tribology field, it can be said that Da Vinci is a pioneer of tribology. He defined two laws of friction, which in 1699 were enunciated by Guillaume Amountons (Hutchings 2016):

1. "The force of friction between two sliding surfaces is proportional to the load pressing the surfaces together."

2. "The force of friction is independent of the apparent area of contact between two surfaces".

Posteriorly, these observations were verified by Charles Augustin Coulomb, who added a third law: "the friction force is independent of velocity once motion starts", and he has also distinguished static friction and kinetic friction.

At the end of 18th century, more developments were done due to the industrialization growth. The principle of hydrodynamic lubrication was made possible due to studies made by Beauchamp Tower (1884), Osborne Reynolds (1886) and N.P.Petroff (1883) (Bhushan 2013c).

Wear is a more recent field of study. It has been developed in midtwentieth century by Ragnar Holm's contributions.

The industrial growth has played an important role in all areas of tribology since the beginning of the 20th century (Bhushan 2013b).

2.2.2 Friction

Friction is defined as the mechanical force that resists movement between two contacting surfaces (Brostow et al. 2003; Theo 2011). It is important to understand that friction is not a property but a system response (Bhushan 2013a).

There are two types of friction that can be distinguished:

• Static friction is the value of the maximum force that is required to initiate motion between two bodies (Bhushan 2013a; Theo 2011) and it is also known as static coefficient of friction (Brostow et al. 2003);

• Dynamic friction, or kinetic friction, is the force required to maintain relative motion and it is also called dynamic coefficient of friction (Brostow et al. 2003).

The movement of the contacting pair can be divided in (Theo 2011):

• Sliding friction occurs in a pure sliding motion between the contacting pair, with no rolling and no spin;

• Rolling friction is generated when a body rolls on a surface;

• Stick-slip is a special form of friction that is due to very slow sliding movements when the contacting pair can vibrate.

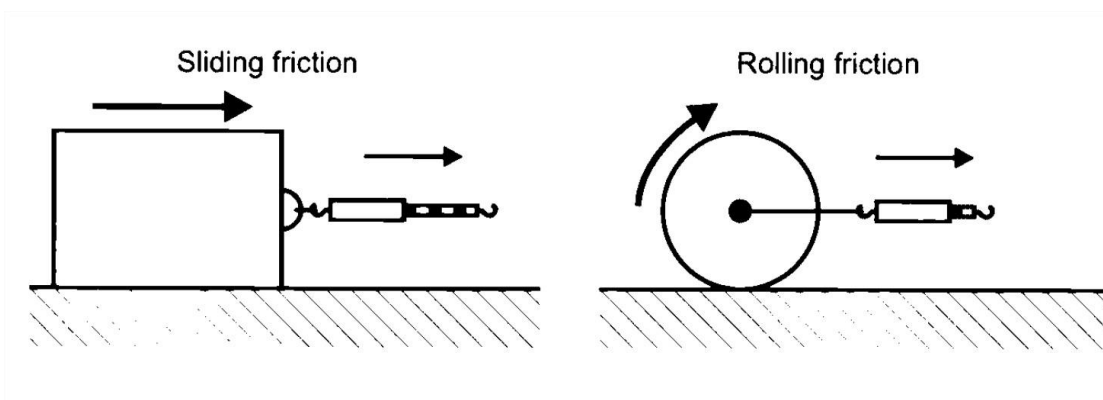Figure 9 shows a representation of sliding and rolling friction mechanisms.

Figure 9 - Schematically representation of sliding and rolling friction mechanisms (Theo 2011).

Friction is not always considered a bad occurrence since it is the friction that allows people to walk or pick up objects, and even in some vehicle brakes, friction is maximized. However, in most other sliding components, such as in bearings, it is undesirable since it leads to wear of surfaces in contact and causes energy loss, in the form of heat or mechanical vibration (Theo 2011; Bhushan 2013a).

2.2.3   Wear

Wear is the surface damage, often involving loss of material, due to interaction between surfaces in contact. As friction, wear is a system response (Bhushan 2013d) and it can be measured in terms of volume, mass or area over a period of time (Theo 2011).

There are four types of wear that can be considered and are presented in Figure 10:

Adhesive wear occurs when two solids are in a sliding contact and the bonding forces between the surfaces on the interface are stronger than the surrounding area in either of the materials (Yamamoto T 1982). Adhesion occurs at contact at the interface and this is sheared by sliding, which may result in the fragment transferred from one surface to another or in the formation of loose wear particles.

Abrasive wear occurs when a hard surface or hard particles slide on a soft surface, causing damage at the interface. There are two types of abrasive wear (Bhushan 2013d):

• Two-body abrasion – The hard surface plays the role of the abrasive.

• Three-body abrasion – A third body, typically a small particle of abrasive, plays the role of the hard surface, causing the abrasive wear.

Fatigue wear occurs when the materials are exposed to a repeat loading and unloading cycles of rolling and sliding. Thus, it is induced the formation of surface and subsurface cracks that will result in the breakup of the surface and in the formation of fragments, after a critical number of cycles (Bhushan 2013d).

Chemical or corrosive wear occurs in a corrosive environment, as in the air, in which the dominant medium is oxygen. The chemical products of the corrosion form a film on the surfaces, which tends to retard the corrosion. However, the sliding action results in the removal of the film and so the chemical attack can continue (Bhushan 2013d).
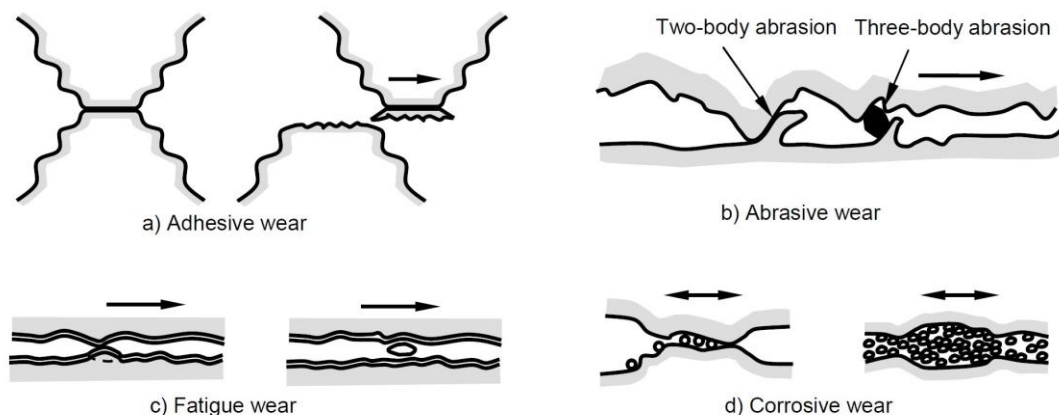

Figure 10 - Schematically represenation of the wear types (Holmberg and Matthews 2009b).

2.2.4 Lubrication

The purpose of lubrication is to reduce friction and wear, introducing a lubricant in order to separate the surfaces. A lubricant can be liquid, gaseous or solid and the most important property of it is its viscosity (Wen and Huang 2012). It is possible identify several types of lubricant regimes, which are presented in Table 2.

Table 2 - Characterization of lubricant regimes (Holmberg and Matthews 2009b).

Regime	Characterization
Dry	The lubricant is a solid
Hydrodynamic	The relative motion of the surfaces results in a pressure within the lubricant, which is high enough to keep the surfaces completely separated
Boundary	A thin lubricant film adsorbs to the surfaces due to the asperity interaction caused by the close movement of the surfaces.
Mixed	It is between the hydrodynamic and boundary lubrication regimes. A thin lubricant film separates the surfaces, but the asperity contacts exists.

A lubrication state has a typical film thickness, but it is not always possible to determine the regime based on this, being used the friction coefficient for that purpose. Figure 11 shows a Stribeck curve, where the dimensionless bearing parameter ($\eta U/p$) refers to the working conditions, being η the lubricant viscosity, U the sliding velocity and p the average pressure (carrying load per length unit) (Wen and Huang 2012).
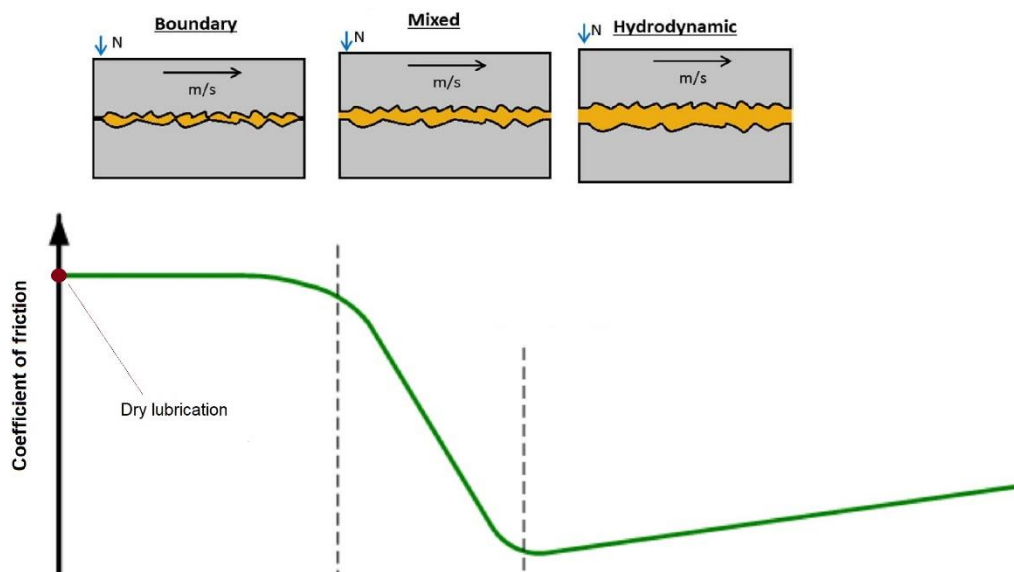

Figure 11 - Stribeck curve and respectively lubrication regimes. Adapted from (W. Robinson et al. 2016).

2.2.5 Applications

In the field of medicine, for the articulating surfaces of artificial joints are used combinations of materials and adverse tissue reactions can be caused by wear. Thus, surface treatments are necessary to improve its wear resistance. Besides this, modular connections are introduced in artificial joints, being constituted by materials as cobalt chromium alloy/titanium so it is necessary to reduce fretting corrosion (Jin et al. 2016). Figure 12 shows the interactions of a hip implant.

A - Articulating surfaces

B - Modular interfaces

C - Fixation interfaces
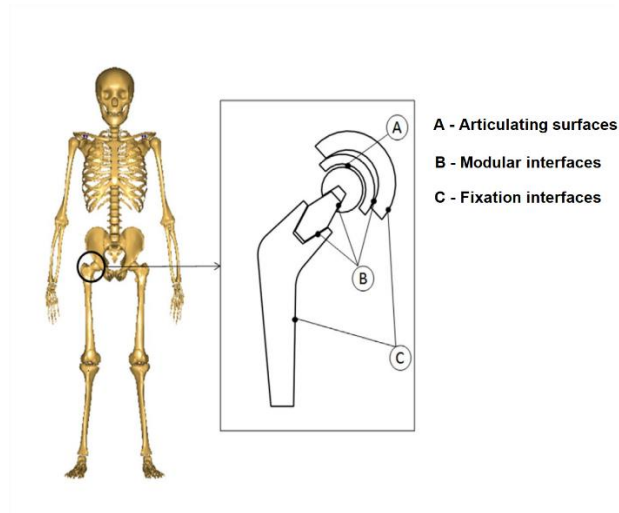
Figure 12 - Interactions of a typical hip implant (Jin et al. 2016).

Dental restorations and implants, due to oral physiological functions, are submitted to friction and wear in the mouth every day, which can result in failure, being necessary take into account the tribological behavior and therefore improve their anti-wear properties. The diagnosis of gastrointestinal tract is an invasive operation since the endoscopy probe is pushed into the human digestive tract, which may cause serious friction damage problems (Jin et al. 2016).

Regarding the spacecraft missions, their success depends on the design and lubrication of the components, which must be capable to withstand the launch environment and the extreme conditions of the space environment (Roberts 2012).

Tribology is not important only to heavy industry. It plays a crucial role in day-to-day life. The process of writing implies good adhesion between the pencil graphite tip and the paper, and the pencil should have the right hardness in order to not break (Bhushan 2013d).

2.3 Tribological Coatings

A tribological coating is a coating that interferes on the properties of the contact pair, usually improving them. This type of coating has applications such as drills, rolling bearings, optical lenses, diesel fuel injectors and pumps (Holmberg and Matthews 2009a).

2.3.1 Formulation

2.3.1.1 Binders

A binder acts as a component to join the elements of the coating and has many functions such as confer adhesion, increase strength, change barrier properties, control electrical properties and enhance durability (McKeen 2006c). In the context of this project the binder selected is a LCP.

2.3.1.2 Fillers

Fillers are typically solid fine particles often used in order to reduce cost, permeability, dissipate static electricity and improve abrasion resistance (McKeen 2006d). In this type of coating, the fillers have a direct impact on the coating after the curing process such as on the reduction of friction, wear resistance and the color. In this work the filler used is Polytetrafluoroethylene (PTFE), which acts as solid lubricant.

2.3.1.3 Additives

Additives generally have functions such as modify or improve the coating properties but sometimes their behavior is not predictable. It can happen that an additive is used and then a second one has to be added in order to correct a problem derivative from the first one. Additives can affect properties of the coating, normally before the cure or during this process for the film formation. They can also have high impact during the application and production processes (McKeen 2006a). In this work, the type of additives selected allows the stabilization of fillers and controlling the thixotropic behavior of the formulation for the application process.

Adhesion Promoters

Adhesion promoters improves the compatibility of certain materials to the substrate to be coated. Typically, these additives are molecules with at least two functional groups, being that one of them interacts with the substrate and the other one reacts with the binder (McKeen 2006a).

Defoamers

Defoamers are an additive used since some surfactants lead to foam formation. Defoamers can prevent the formation of the foam or eliminate its presence if it is already formed (McKeen 2006a).

Flash Rust Inhibitor

The purpose of a flash rust inhibitor is to reduce the velocity of the oxidation reaction and it is only necessary if the formulation contains water. This reaction is a consequence of the

oxygen and water combined with the surfactants that attack unprotected steel surfaces quickly (McKeen 2006a).

Rheology Modifiers

These additives enable the adjustment of the behavior of the formulations during the process, allowing an adequate viscosity for application, storage and stability of the coating.

Dispersants/Surfactants

In coating formulations, it often happens that there is a certain incompatibility between components, being necessary use a dispersant to stabilize them. The surfactants are a type of dispersants, which include the wetting agents. (McKeen 2006d). The latter is a substance that decrease the surface or interfacial tension and promotes the wetting (Müller and Poth 2011).

2.3.1.4 Carrier

A carrier is the solvent system and for the determination of which one must be used, there are several factors to be considered (McKeen 2006f):

- Rheology and viscosity of the formulation
- Boiling point and evaporation rate
- Compatibility of the components with the solvent
- Dispersion stability
- Surface tension
- Safety issues

During the present work the carriers used are N-methyl-2-pyrolidone (NMP) and water.

2.3.2 Surface treatment of the substrate before coating

In order to guarantee a successful application of the coating, it is necessary a preparation of the surface before the application.

An important factor to consider is the adhesion of the coating to the substrate, which can be assured through the removal of impurities and by increasing surface area. The cleaning process of the surface can be done by chemical or physical processes and the increasing of surface area can be done by providing roughness to this, having several ways to do it, as grit blasting (McKeen 2006g).
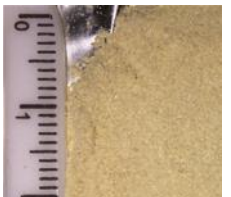
3 Materials and Methods

During the development of the present work, several equipment and materials were used in order to study and understand the concepts involved and then obtain results to support them, which will be presented posteriorly. In this chapter, the presentation of the materials, the operating mode of the equipment and relevant procedures are described.

3.1 Materials

The polymer used during the present work is Liquid Crystal Polymer (LCP) and there were tested four different grades of it, being some aspects of their physical appearance presented in Table 3. Since these products are supplied by different companies under confidentiality agreements, the information about them is limited.

Table 3 – Characterization of LCPs.

	A	B	C	D
Condition	Powder	Pellet	Powder	Powder

The filler selected was Polytetrafluoroethylene powder (PTFE) Zonyl MP1600 provided by Chemours, which also acts as a solid lubricant.

As additives, there were used surfactants and rheological modifiers available in Tribochem's Laboratory. Due to confidentiality agreement, the commercial name of the additives cannot be declared.

3.2 Physico-chemical characterization

Thermogravimetric analysis (TGA) is a technique that measures the loss of mass of a sample as a function of temperature or time, in order to understand the stability of the material. This test is performed during a controlled temperature program and in a controlled atmosphere. The latter can be inert, such as nitrogen, or oxidizing, such as oxygen. The test was performed on a Netzsch TG 209 F1 with crucibles made of Pt-Rd and the samples were heated until 1100 ºC at a rate of 10 ºC·min^{-1}.

Differential scanning calorimetry (DSC) is a thermal analysis in which the heat flow rate between a substance and a reference is measured as a function of temperature, during a controlled temperature program. This technique allows the determination of the glass transition, melting and crystallization temperatures and the related heat flux variations. In this work, there were used crucibles made of aluminium and the temperature program is presented in Table 4. The test was performed on a Netzsch Polyma DSC214.

Table 4 – Temperature program of DSC analysis.

Step	Temperature range	Ramp up
1	-20 °C to 450 °C	20 K·min^{-1}
2	450 °C to -20 °C	20 K·min^{-1}
3	-20 °C to 450 °C	20 K·min^{-1}

Fourier-transform infrared (FTIR) spectroscopy is an analytical technique where infrared radiation passes through a sample allowing the determination of which fraction of incident radiation is absorbed or transmitted at a particular energy. Thus, it is possible to identify different chemical structures of the sample. The test was performed on a Brucker Vertex 70 FTIR with attenuated total reflection (ATR) module and the number of scans defined was 256.

X-ray diffraction (XRD) analysis is made using X-ray to evaluate the crystalline nature of the material. This occurs by measuring the X-ray diffraction from the planes of atoms within the material. XRD measurements were performed at IFIMUP-IN facilities, in a Rigaku SmartLab diffractometer that operates with 9 kW power (45 kV and 200 mA) and a Cu source with a wavelength λ = 1.540593 Å in a Bragg-Brentano geometry. All the samples are measured at room temperature over the range 2θ = 5–100°.

Scanning Electron Microscopy/Energy Dispersive X-Ray Spectroscopy (SEM/EDS) allows an observation of the materials that is not possible by naked eye. Besides that, it is possible to identify elements that are present in the sample by imaging regions. For this analysis, the samples are covered by gold sputtering with the purpose of providing electrical conductivity, which some materials do not have, such as polymers. This method uses a beam of electrons that focuses on the sample and interacts with the atoms on it. There are electrons that come out of the sample in the moment that the beam focus on it and are these ones that allow the production of a SEM image. There are two operation modes of this equipment: Secondary Electrons Detector (SED) and Backscattered Electron Detector (BSD). The SED mode is used to produce a topographic SEM image while the BSD mode takes in consideration the atomic mass

and so heavier elements appear brighter than the lighter ones. The test was performed on a SEM Phenom XL.

3.3 Coating formulation

Before the formulation, it is necessary to solubilize LCP. In the solubilization process, the solvent is heated under agitation in a glass vessel and then LCP is added. The agitation must continue about four hours, in order to allow a total solubilization, being the temperature controlled by the heating source while a condenser avoid the solvent evaporation. After that, the solution is filtered to remove non-solubilized particles.

Rotor-stator provides a dispersion of two phases through a high velocity and a mechanical contact. The equipment is constituted by two parts as the name itself indicates, the rotor and the stator, being the latter static while the rotor has a rotational movement. An important characteristic of the equipment that makes possible the dispersion is the high shear, which allows the separation of particle agglomerates. However, taking into account the latter situation, there is a need to control the temperature since the high shear leads to an increase of it. The equipment mechanism is presented in Figure 13.
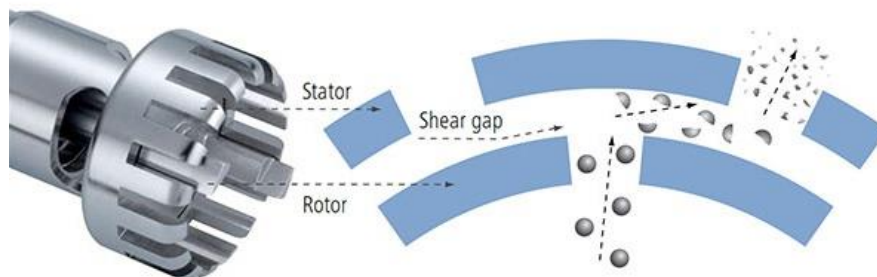

Figure 13 - Rotor-stator dispersion mechanism ("Laboratory-Equipment").

3.4 Surface preparation

For this work, the substrate selected was common steel alloy sheets with 200 x 100 mm size and 0.9 mm thickness. Initially, a pyrolysis is performed on the steel sheets at the cure temperature of the coating to remove all the contaminants. Then, a blasting process occurs with projection of aluminium oxide. The latter is done in order to promote a controlled roughness, assuming values of roughness average (R_a) around 2 µm to 4 µm.

3.5 Coating application and cure

During the development of the present work, a conventional spray gun is used to apply the coating formulation. The formulation goes to the gun nozzle by gravity where is atomized due to a set of air orifices, allowing the liquid to form a spray. The flow of the formulation is

controlled by a needle valve. The pressure of the air used for atomization is also controlled. Figure 14 shows a conventional spray gun and them constituents.
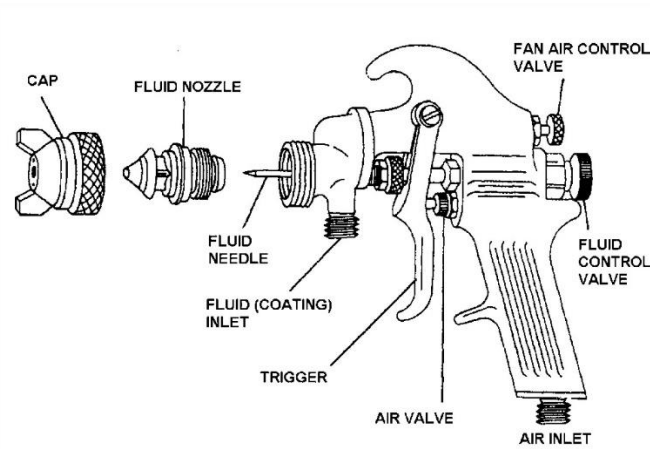

Figure 14 - Schematically representation of a spray gun (McKeen 2006b).

After the coating application, the substrate goes to an electric forced-convention oven in order to be cured in a curing cycle of 380 ºC for 15 minutes.

3.6 Mechanical and tribological characterization

The thickness measurement is made through a non-destructive thickness gauge that detects the substrate, after an initial configuration and so it can measure the distance between the top of the coating and the substrate. The measurement is made in several points of the coating in order to have an average. The measurement was performed on an Elcometer 456 inductive coating thickness gauge with dual sensor (Ferrous/Non-ferrous).

The adhesion test made during the present work is the cross-hatch test, which consists in cutting a lattice pattern into the coating already applied and cured. The procedure used is an adaptation of the standard ASTM D 3359 – 97. This test is made with a x-cut and after that the cutting zone is scrubbed in order to evaluate if the coating remains in the substrate or if there are some fragments that release from it.

The tribometer is an equipment that measures properties of a material such as friction. There are several tests to do in this equipment and the one used was the linear reciprocating test ball on plate, using a GCr15 steel ball with 10 mm diameter and a coated steel plate with a thickness of 0.9 mm. This test consists on a ball making a defined distance, at a defined speed and load, in a coated plate while the equipment is measuring the coefficient of friction. The coefficient of friction is the ratio between the tangential friction force and the normal load *(Holmberg and Matthews 2009b)*. Table 5 shows the conditions of the tests made. The test was performed on a Bruker UMT-3 tribometer, presented in Figure 15, with a linear reciprocating module.

Figure 15 – Tribometer, at left ("Bruker"). Plate on ball test, at right.

Table 5 – Conditions of the ball on plate test.

Load / N	Sliding velocity / mm·s^{-1}	Stroke / mm	Time / h	Sliding length / m
5	5	2	3	54
5	10	2	1.5	54
10	5	2	3	54
10	10	2	1.5	54

The profilometer is an equipment that measures the roughness of a surface and the wear profile since it evaluates the surface topography profile in a linear direction. This device contacts with the sample and in the present work it is used in order to evaluate the worn track after the tribological test, allowing the calculation of the volume that was lost during the test. The test was performed on a Hömmel Tester T4000 bench top.
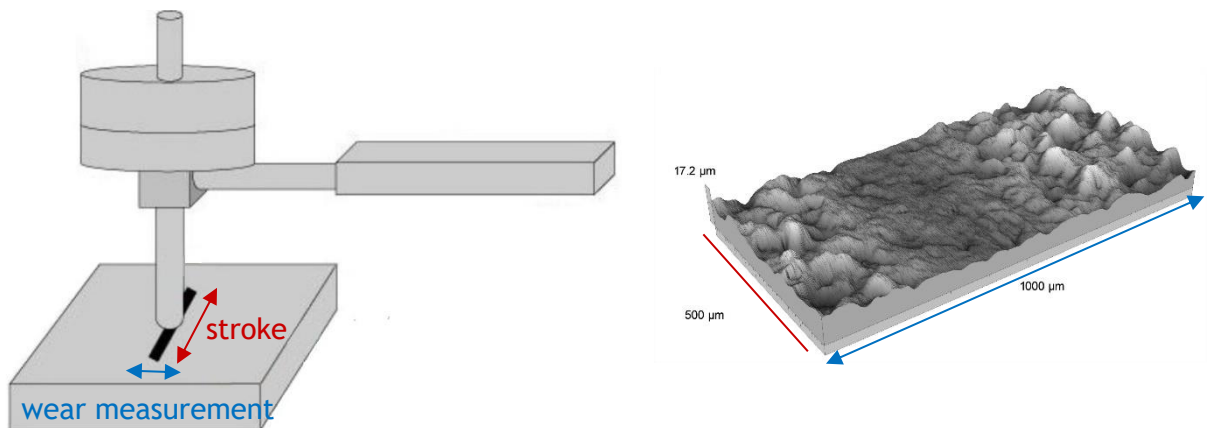
Figure 16 – Representation of the section analysed by the profilometer. Adapted from ("Azonano").

The removed volume obtained by the software corresponds to a section of 500 μm of the total track so it is necessary multiply it for 4 in order to obtain an estimate value of the total volume removed in the track, which corresponds to 2 mm. To calculate the wear rate, $\dot{W}$, it is used the equation (1), where V_r is the removed volume (mm³), L is the load applied (N) and d is the sliding distance (m).

$$\dot{W} = \frac{V_r}{L \times d} \qquad \left(\frac{mm^3}{N \times m}\right) \qquad\qquad (1)$$

4 Results and discussion

The work developed has four main steps. Firstly, it was made a physico-chemical characterization of the LCPs. Then, the solubilization of them was tested and after, the formulation of the coating was performed, using the previous solution. Lastly, it was made a tribological characterization of the coating.

4.1 Physico-chemical characterization of LCP as raw material

In order to understand one of the characteristics that makes LCP an unique material, its thermal stability, TGA and DSC analysis were made. Figure 17 and Figure 18 show TGA results.
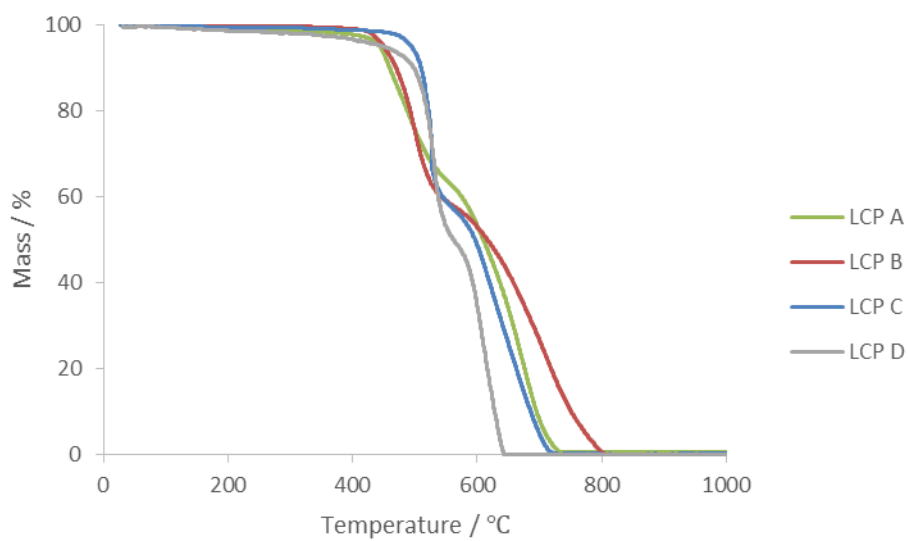
Figure 17 – TGA of LCPs tested in O_2.
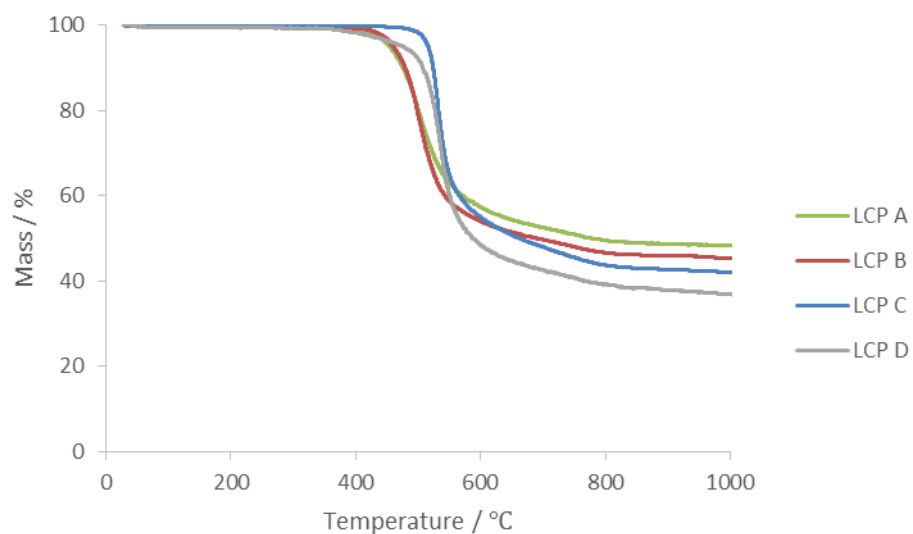
Figure 18 – TGA of LCPs tested in N_2.

As it can be seen, LCPs C and D have a higher decomposition temperature so theoretically these two polymers would be the best choice for the present work. The test performed in O_2 allows the prediction of the decomposition temperature of the polymer during the cure process as well as to verify if there is oxidative decomposition. Therefore, TGA runs were repeated in an inert environment, N_2, in order to observe the real decomposition temperature of the polymers and the results are presented in Figure 18.

Through the TGA software it is possible to get the value of onset temperature, which is the temperature at which the material starts decomposing. Table 6 shows the onset temperatures of each LCP in an oxygen medium and in an inert one. Taking into account Figure 18, it is possible to verify that in an inert environment all the LCPs have only one step of degradation. Through the observation of the onset temperatures, it is verified that differences between the two environments are not significant. Thus, the first step observed in Figure 17 is related to the thermal decomposition while the second one is related to oxidative reactions.

Table 6 - Onset temperatures of LCPs in O_2 and N_2.

	LCP A	LCP B	LCP C	LCP D
Onset temperature in O_2 / °C	439.2	462.1	513.4	501.7
Onset temperature in N_2 / °C	437.3	458.0	527.5	507.0

Regarding DSC analysis, observing Figure 19 it is possible to observe the glass transition temperature (T_g) for LCPs A and B and the melting temperature (T_m) temperature for LCPs C and D. These values are presented in Table 7.
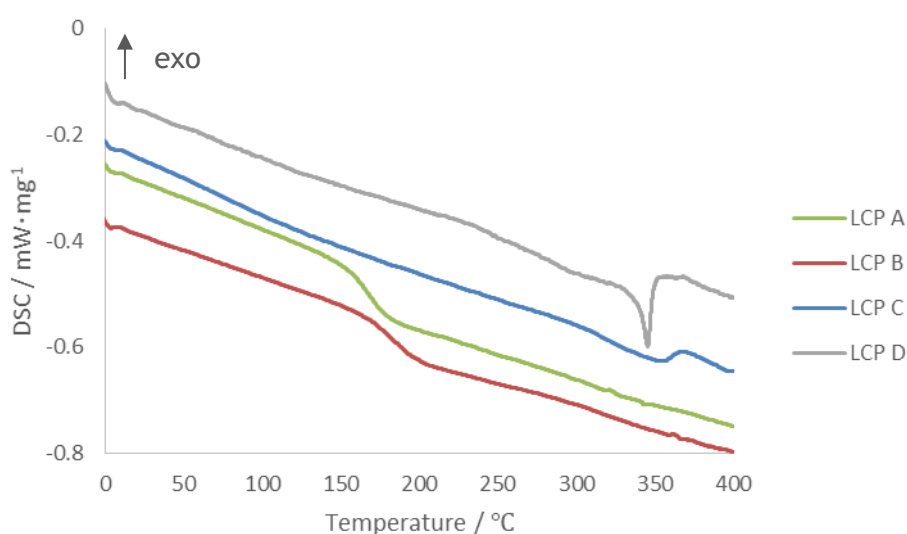

Figure 19 - DSC of LCPs tested.

Table 7 – Relevant temperatures of DSC analysis.

	LCP A	LCP B	LCP C	LCP D
T_g / °C	168	183	_____	_____
T_m / °C	_____	_____	355*	345

*it is not certain that it is a T_m

Through the observation of Figure 19 it is possible to see a slightly slope between 100 °C and 200 °C, which can correspond to a T_g although it is not certain. These results show that LCPs C and D are probably thermotropic, since they present a melt transition, which explains the fact that they are not soluble.

4.2 Coating formulation and application

4.2.1 Solubilization and dispersion of LCPs

After the characterization of LCPs, there were performed solubilization tests and the results are presented in Table 8.

Table 8 - Conditions of the solubilization tests.

	Conditions	Result
LCP A	15 % wt in NMP	• Homogeneous solution
LCP A	20 % wt in NMP	• Homogeneous solution that gelified in one day
LCP A	35 % wt in NMP	• Homogeneous solution that gelified in one day
LCP B	15 % wt in NMP	• Homogeneous solution
LCP B	20 % wt in NMP	• Homogeneous solution that gelified in one day
LCP B	35 % wt in NMP	• Homogeneous solution that gelified in one day
LCP C	35 % wt in NMP	• Did not solubilize
LCP D	35 % wt in NMP	• Did not solubilize

As it can be seen, LCPs A and B were the only ones that achieved a homogeneous solution. Through the solubilization results it is possible to observe that for a lower solid content of LCP, the solution remains stable while for higher solid content the solution gelifies, increasing its viscosity in a way that does not allow its stability and application.

In order to obtain results from the LCPs that previously did not solubilize, it was tested the dispersion of them, being the results presented in Table 9.

Table 9 - Conditions of the dispersion tests.

	Conditions		Result
LCP C	25 % wt in water		• LCP C powder deposited
LCP D	15 % wt in water		• Apparently homogeneous dispersion
	15 % wt in NMP		
	25 % wt in water		• Not-homogeneous dispersion, with agglomerates

Regarding LCP C, it was not possible to reduce the particle size in the rotor-stator and therefore the powder deposited. For LCP D, with a higher solid content, the dispersion did not result since it had agglomerates. With a lower solid content, apparently it was achieved a homogeneous dispersion.

4.2.2   LCP analysis after solubilization

In order to verify if the solubilization modified the LCP, a TGA of the solution was performed. For that, a small quantity of the solution was heated during 15 minutes at 270 ºC, to remove the solvent (NMP), which presents a boiling temperature of 202 ºC, and obtain a solid sample. Figure 20 and Figure 21 show a comparison for LCPs A and B as supplied with the ones dried from respectively solutions after the heating process described before.
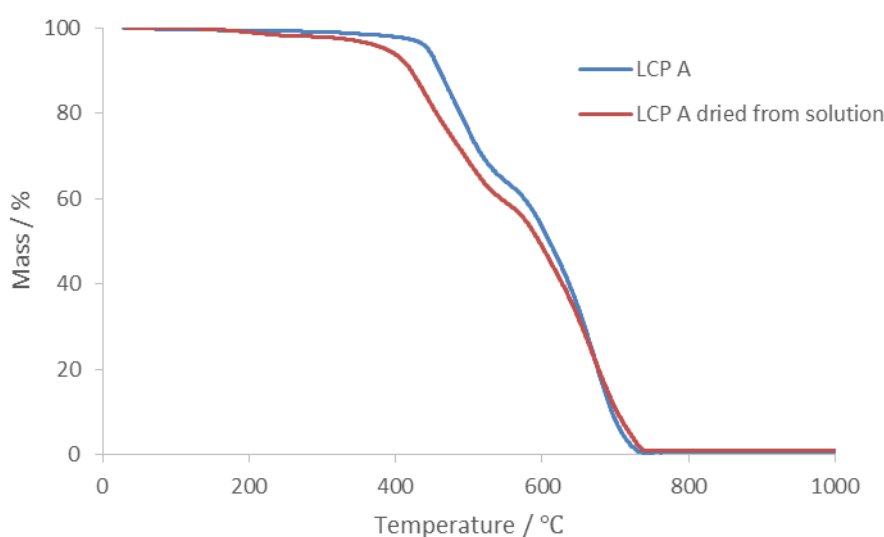
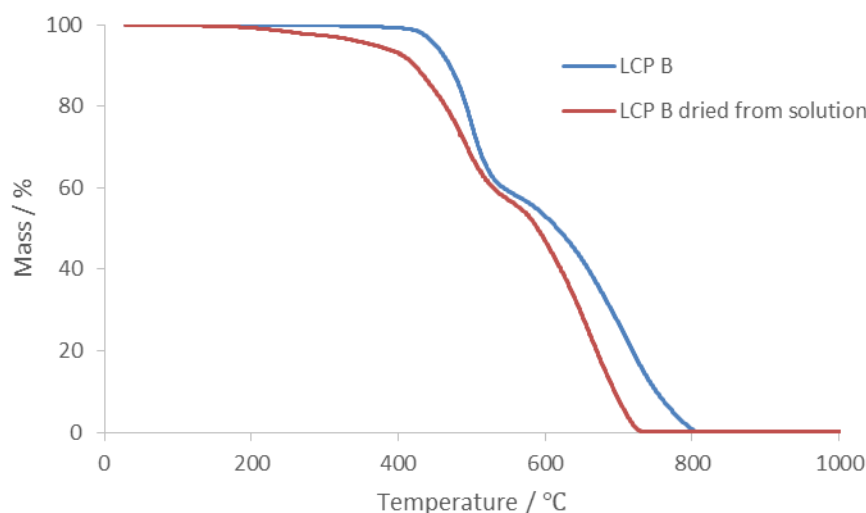*Figure 20 – TGA in O_2 of LCP A as provided and LCP A dried from solution.*

Figure 21 –TGA in O₂ of LCP B as provided and LCP B dried from solution.

As it can be seen, there is a difference between the solutions after dried and the respective LCPs, which may mean that the material became less crystalline after being dried from the solution, leading to decomposition at a lower temperature. On the other hand, besides the sample has been dried above the boiling temperature of the solvent, it can contain traces of solvent that cause the differences observed.

Taking into account the TGA results and the solubilization and dispersion tests, the two best options would be LCP A and B. However, being LCP B a pellet and LCP A powder, the first was selected since it allows a better handling and cleaning for the purpose of laboratory work.

In order to verify the presence of some typical functional groups of LCPs, a FTIR analysis of LCP B was performed. Figure 22 shows the results of this analysis for LCP B.
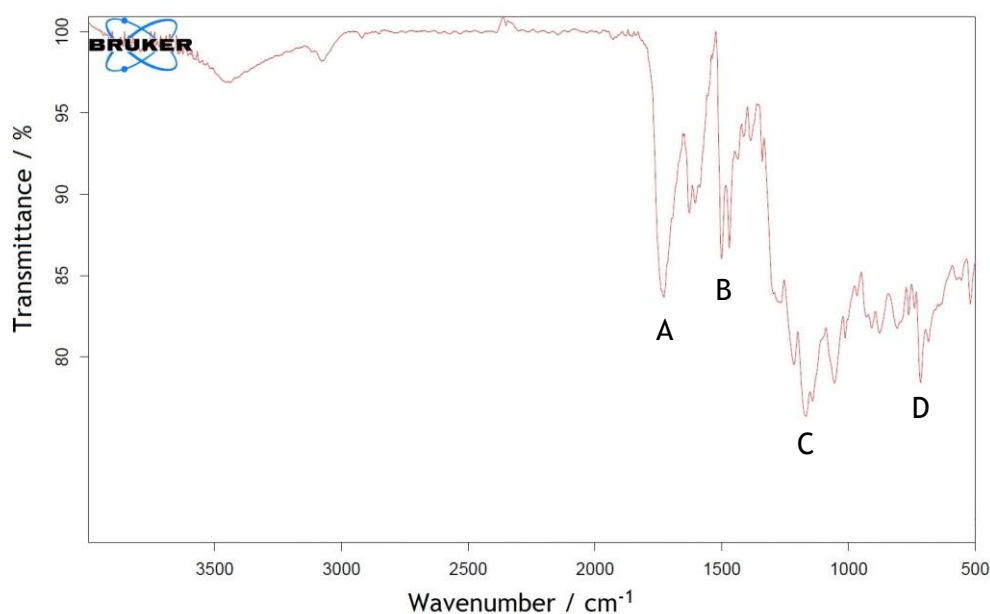
Figure 22 – FTIR analysis of LCP B.

Table 10 presents the analysis of some peaks indicated in the previous figure. Through this analysis, it is possible to confirm the presence of some functional groups that can constitute LCPs, as it was mentioned in Chapter 2.

Table 10 – Analysis of some FTIR peaks.

	Wavenumber / cm^{-1}	Group
A	1728.67	C=O
B	1500.67, 1469.95	C=C aromatic ring
C	1167.45, 1142.17	C-O-C
D	715.87	C-H bending

At 1550.67 cm^{-1} and 1469.95 cm^{-1} it is observed a C=C chemical bond from an aromatic ring, with is according to the basic structure of LCPs. At 715.87 cm^{-1} it is observed the presence of a C-H bond, which can be relating to the aromatic ring.

4.2.3 Coating formulation

Taking into account the results obtained from the solubilization and dispersion tests, there were performed four formulations, based on LCPs B and D. The components of them are presented in Figure 23.
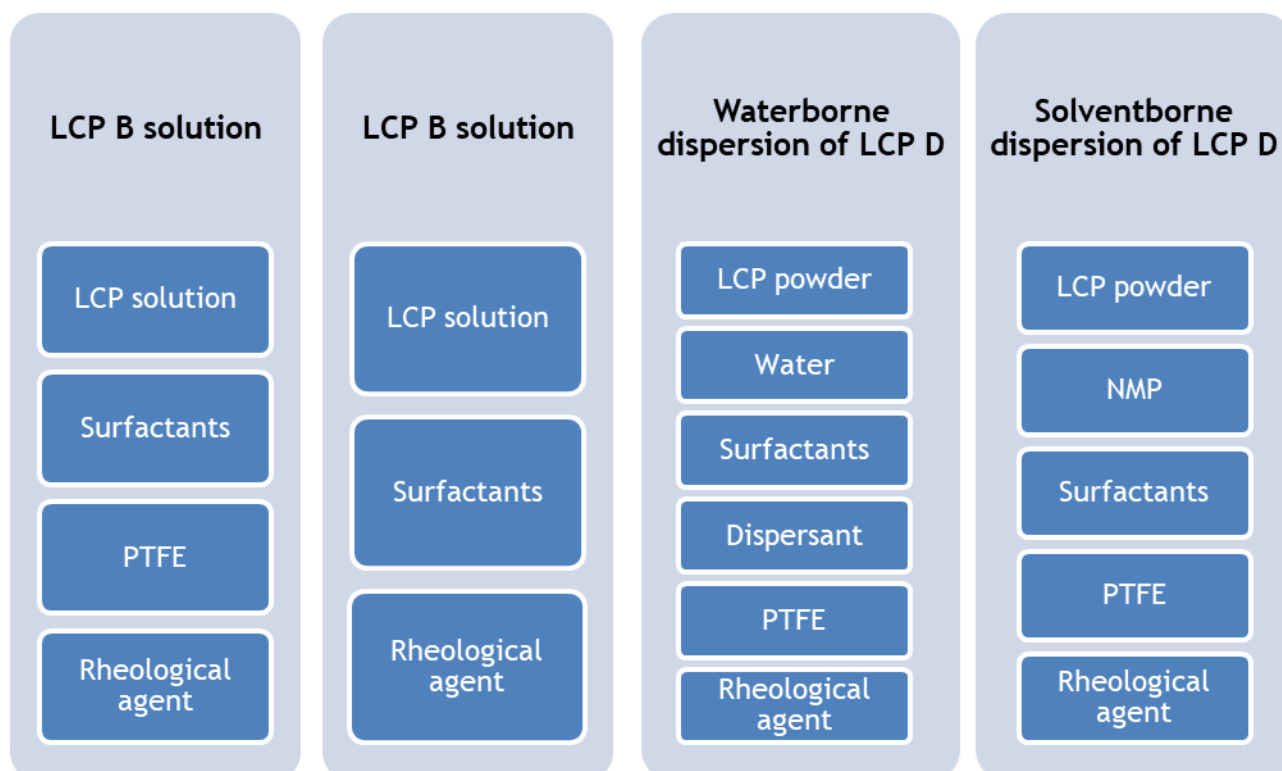
*Figure 23 - Components of the formulations performed.*

However, during the application process of the LCP D formulation based on a waterborne dispersion, it was verified the presence of agglomerates, as it will be discussed later. Thus, it was noticed the same problem with the agglomerates in the LCP D formulation based on a solventborne dispersion and so this one was not applied.

4.2.4   Coating application and cure

Two coating formulations were produced using LCP B, at 15 % wt. One of the formulations contains PTFE while another is free of it. The result after application and curing can be seen in Figure 24 and Figure 25. Regarding the one with PTFE, it was applied in two steel plates with the same dimensions.

Figure 24 – Photograph of LCP B coating.
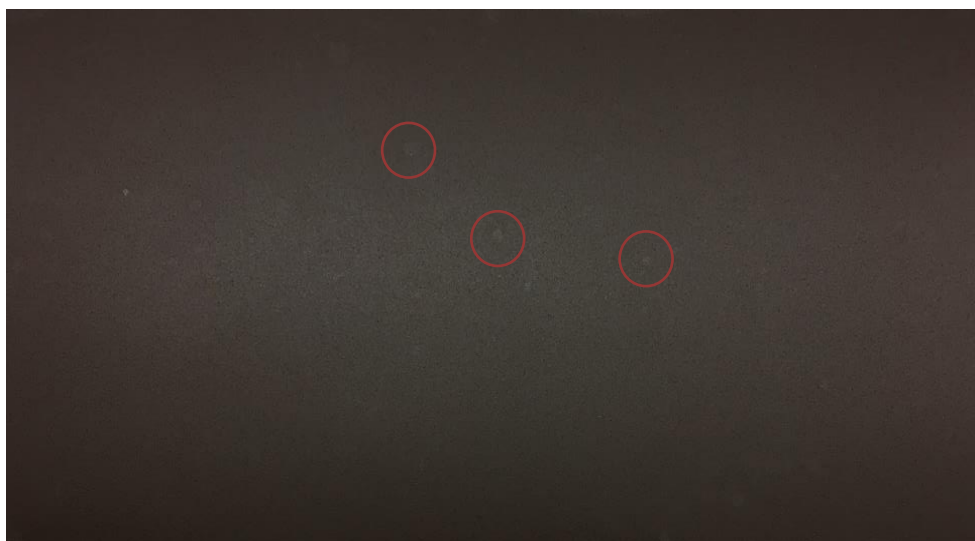
Figure 25 – Photograph of LCP B coating containing PTFE.

Taking into account the previous two figures, it is possible to observe some white spots that are probably derived from a bad wetting since the formulation was applied in laboratory conditions by non-specialized operators. On the other hand, the quantity of surfactant may need to be adjusted.

Figure 26 shows the waterborne dispersion coating of LCP D. Through the observation of the coating after the cure process, it is possible to see some white spots. These ones are due to agglomerates that, as already mentioned, were verified during the application of the formulation.
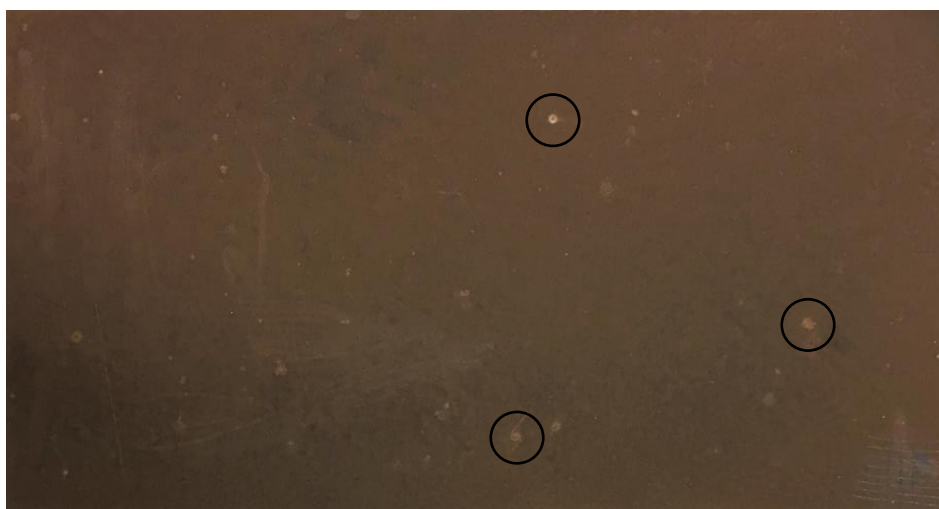
Figure 26 – Coating of LCP D waterborne dispersion.

The coating thickness measurements are presented in the Table 11. For characterization purposes, it was selected the LCP B and LCP B + PTFE (Plate 2) due to the similarity on the thickness to not include more variations on the analysis.

Table 11 – Thickness measurements of each coating after the cure process.

	LCP B	LCP B + PTFE (Plate 1)	LCP B + PTFE (Plate 2)
Thickness / μm	15.95 ± 1.38	27.51 ± 1.69	16.66 ± 1.78

4.2.4.1 SEM analysis

Figure 27 shows some SEM images with different magnification of the LCP B coating that does not contain PTFE.
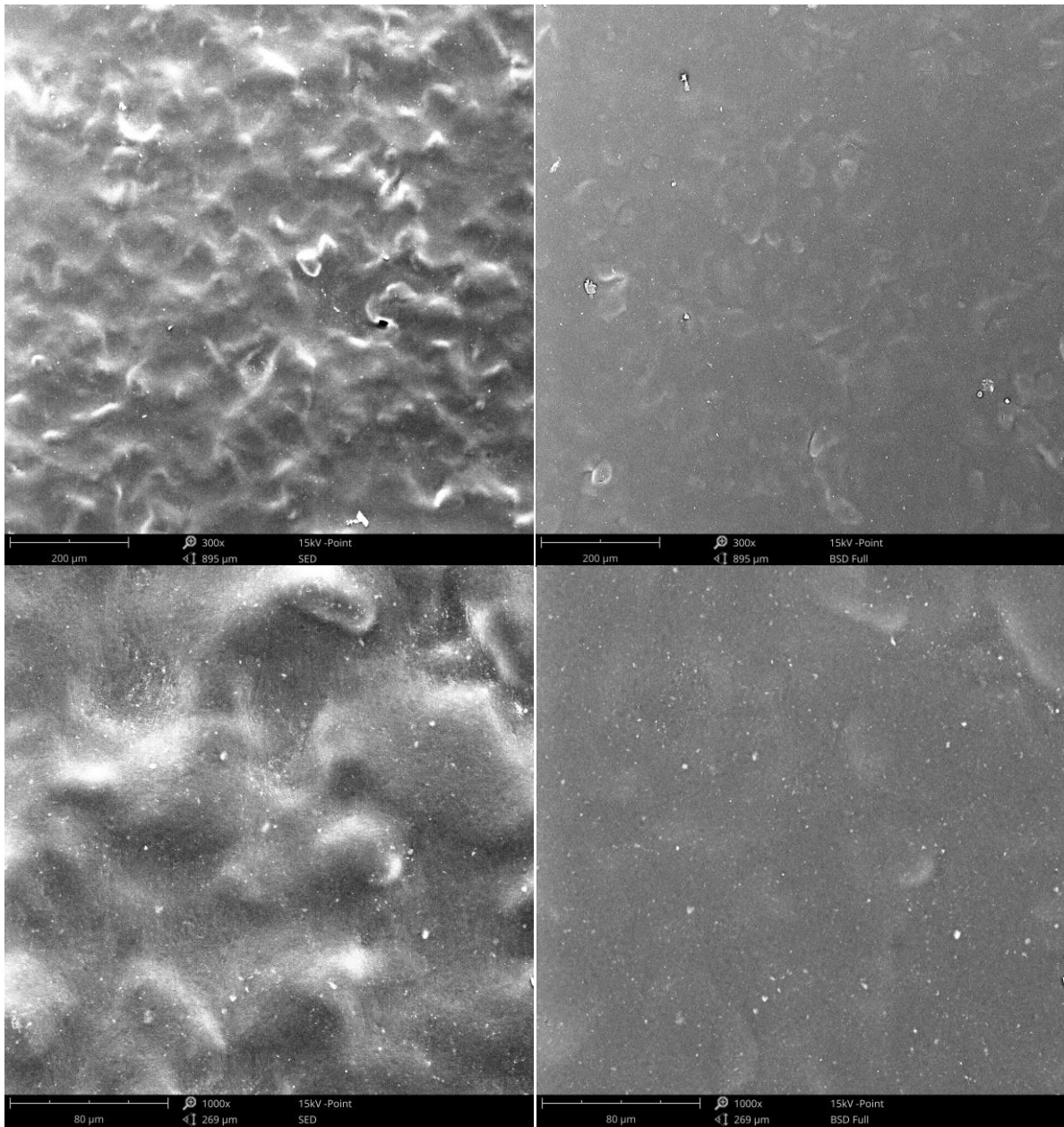
Figure 27 - SEM images of LCP B coating.

As it can be seen, there are some white spots and a magnified image of them can be observed in Figure 28.
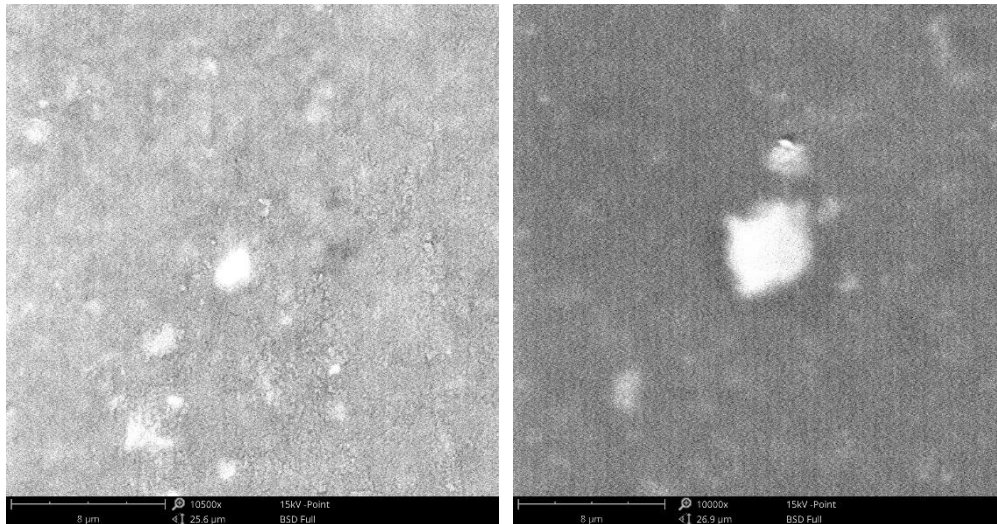
Figure 28 – SEM images of white spots in LCP B coating.

It is observed the existence of Zn, K and Si on the white spots, being this information obtained through the elemental mapping in SEM/EDS analysis, presented in Figure 29. It is possible that these elements are constituents of the rheological agent used in the formulation. On the other hand, they might be contaminants of the system.
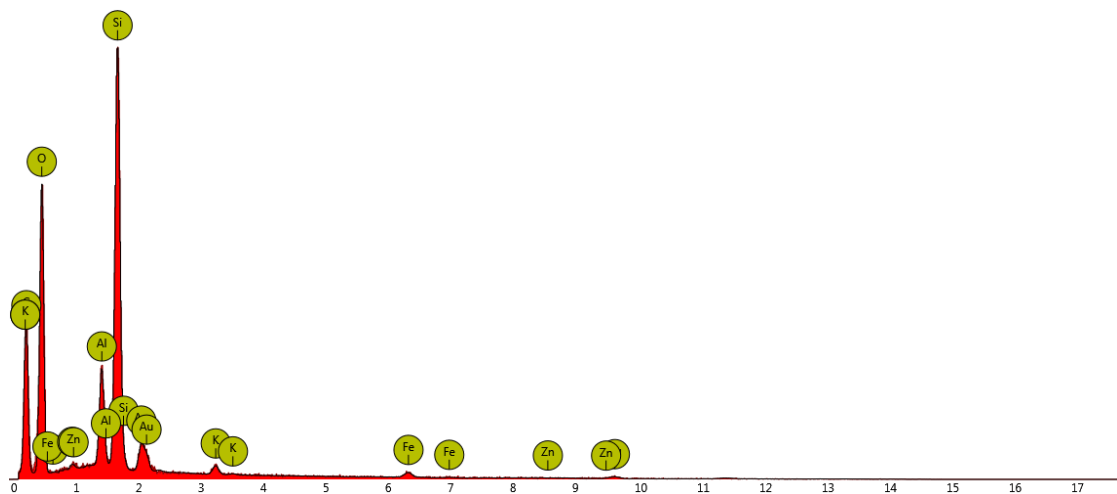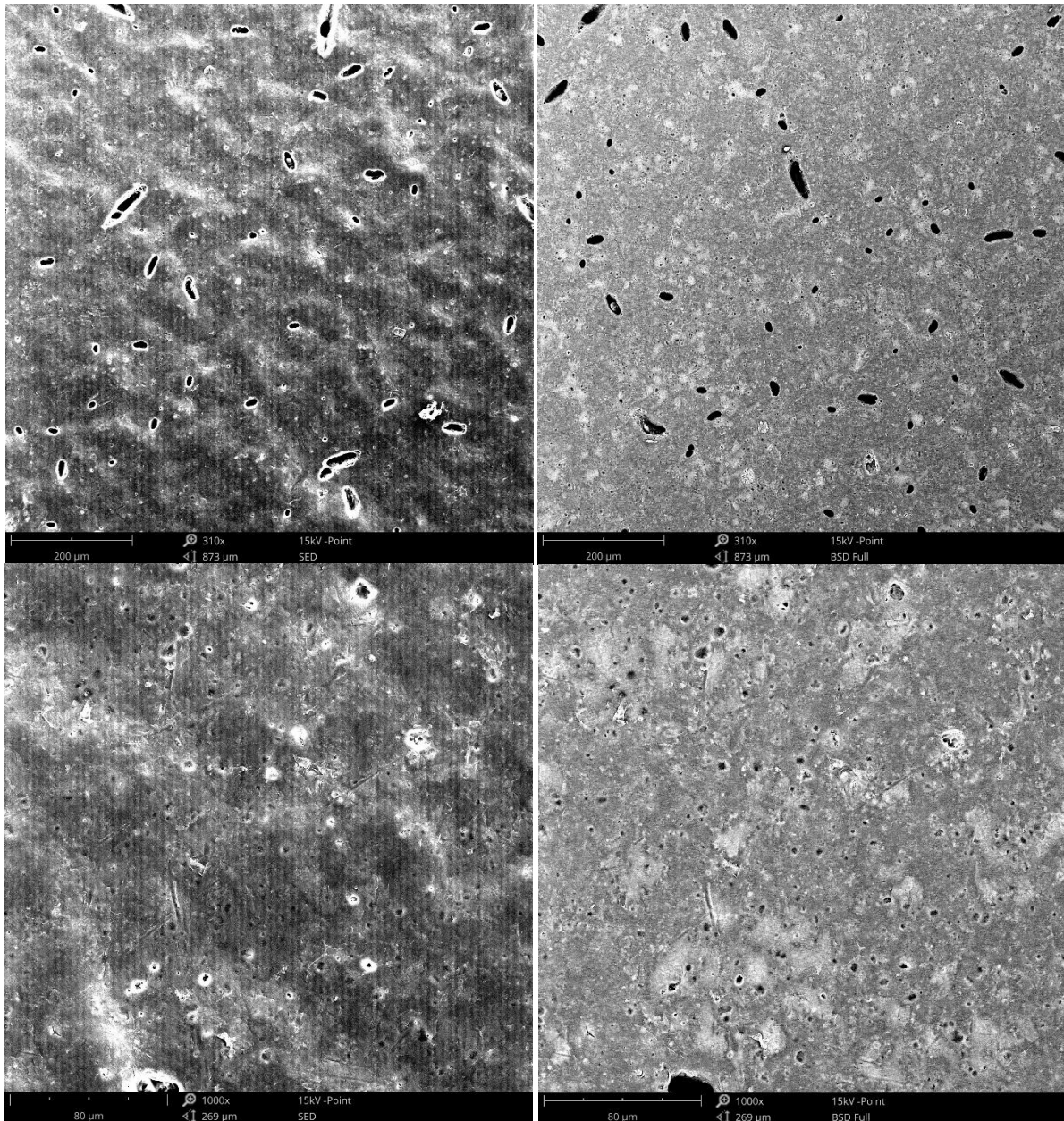

Figure 29 – Elemental analysis of the white spots present on LCP B coating.

Figure 30 shows some SEM images with different magnification of the LCP B + PTFE coating.

Figure 30 – SEM images of LCP B + PTFE coating.

As it can be observed by the observation of Figure 30, there are holes in the coating that contains PTFE, while on the coating without PTFE they are not present (Figure 27). Both coatings were cured at the same time, with the same conditions since they were positioned at the same high in the oven. It might be that the heat source in the oven was closer to the coating with PTFE and therefore it was promoted a faster evaporation of the solvent, leaving the holes observed. On the other hand, PTFE has a high melt viscosity at the cure temperature (380 °C), which causes the formation of holes (E. Banks et al. 1994). Taking into account these factors, the cure process must be optimized. Figure 31 shows a SEM image of the holes, at left, and the fibrillation of PTFE, which is a common phenomenon (McKeen 2006e), at right.
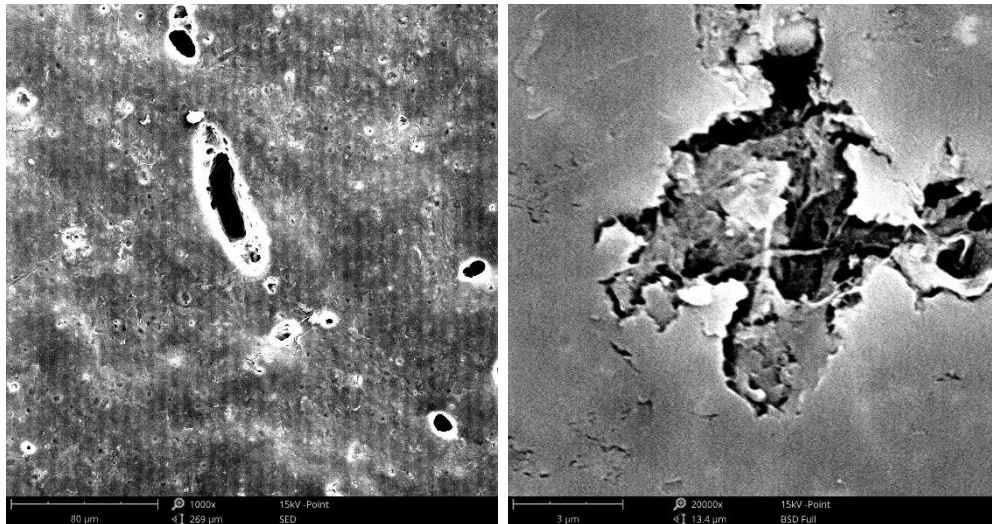
Figure 31 – SEM images of LCP B + PTFE coating cured. At left, a hole; at right, PTFE fibrillation.

4.2.4.2 XRD analysis

In order to evaluate the crystallinity of LCP B, a XRD analysis was made to compare it with other found in the literature. Taking into account that there is a wide range of LCPs, they present different peaks according to their structure. Through the research made, it was possible to found a XRD spectrum that contains some similar peaks to LCP B. However, the LCP found is unidentified regarding its chemical structure, although it is identified as a LCP. The XRD results for LCP B and for the one presented in the literature can be seen in Figure 32.
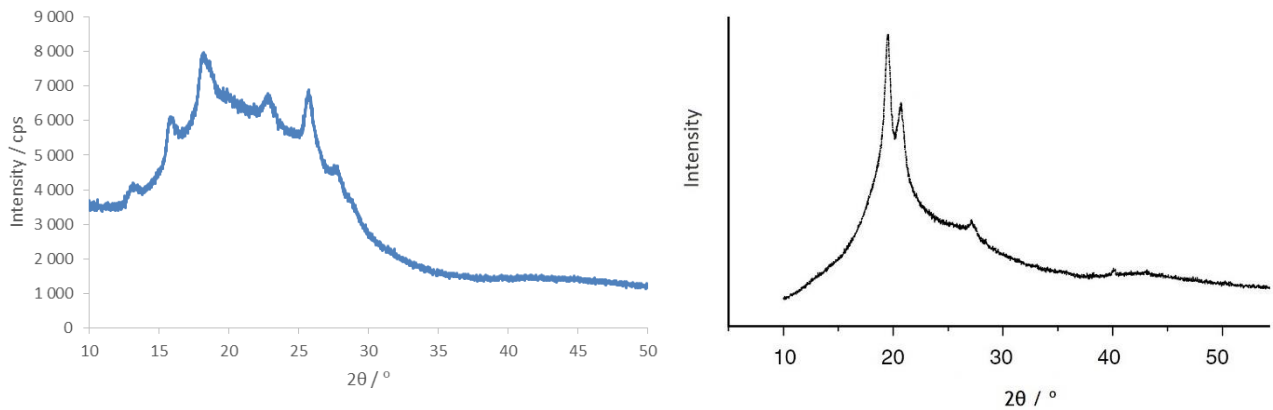

Figure 32 – XRD analysis: at left, LCP B; at right, a LCP found in literature(P. Jose and Joseph 2012).

To evaluate the crystallinity of the coatings according to LCP B crystallinity, XRD analysis of the coating was made and it is presented in Figure 33.
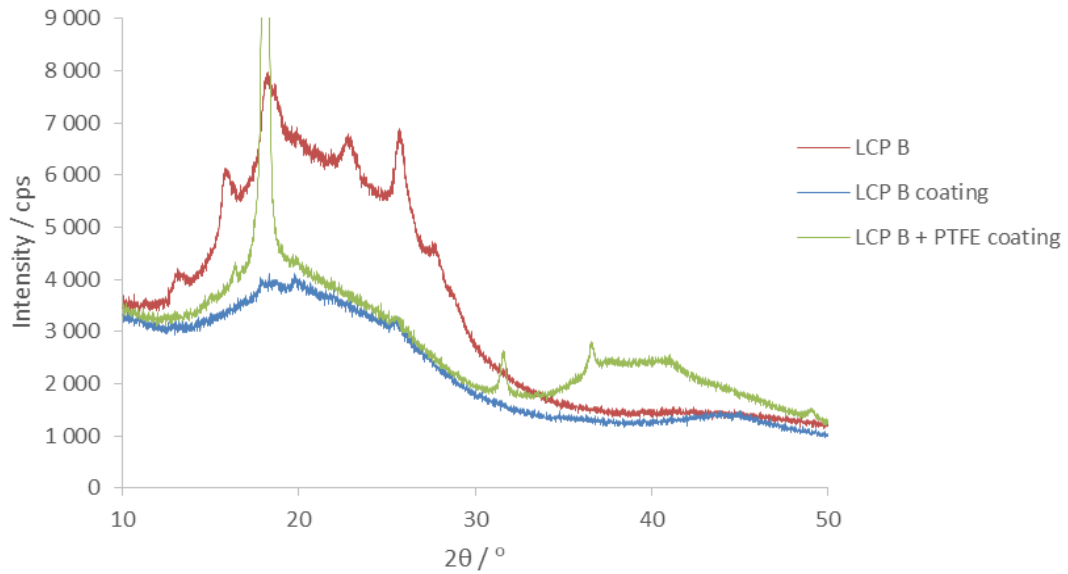
Figure 33 – XRD analysis of LCP B and LCP B coatings.

As it can be observed, when LCP B is incorporated in the formulation and cured to form the coating, there is a decrease in crystallinity, since the peaks present lower intensity and even are badly defined. Figure 34 shows the XRD analysis of the coating that contains PTFE, at left, and a XRD analysis of PTFE, at right. It is possible to observe one high intensity peak and two low intensity peaks, which is according to the studies already made (Das et al. 2006; Lebedev et al. 2010).
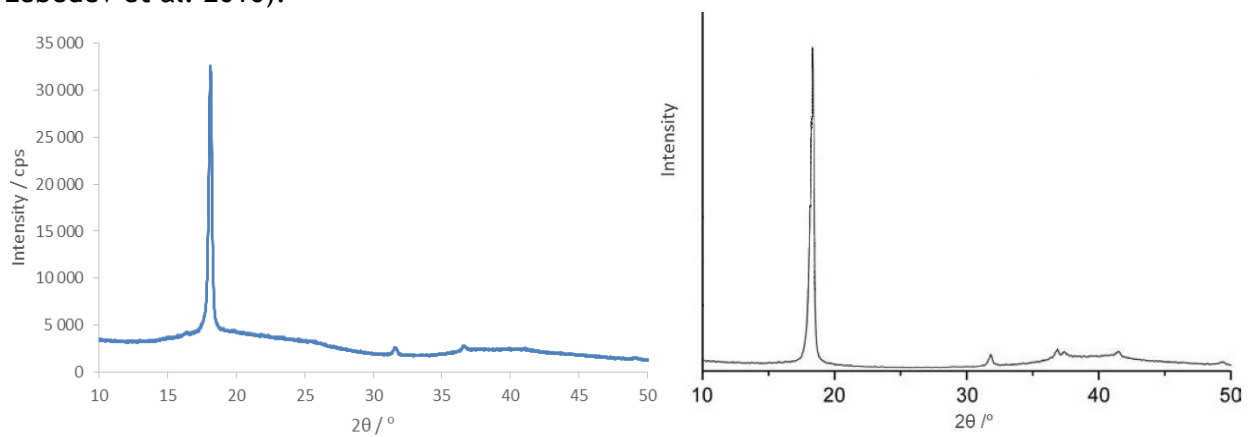

Figure 34 - XRD analysis of LCP + PTFE coating, at left. XRD analysis of PTFE, at right. Adapted from (Das et al. 2006).

4.2.5 Coating adhesion

Before the tribological characterization, it was necessary verify if the coating adhered to the substrate, so a cross-hatch test was made, being presented in Figure 35. As it can be observed, LCP B coating with and without PTFE showed a good adhesion since there was not fragments released.
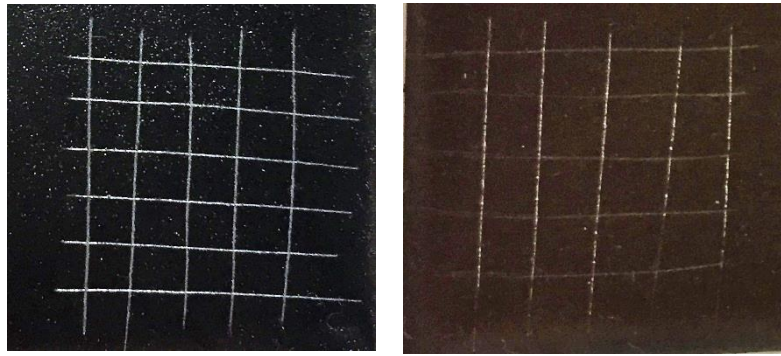
Figure 35 – Cross-hatch test. At left, LCP B without PTFE; at right, LCP B + PTFE.

4.3 Tribological characterization

4.3.1 Effect of PTFE

In order to evaluate de effect of the PTFE on the coating performance, the coefficient of friction of the coatings LCP B and LCP B + PTFE was compared in Figure 36 and Figure 37 for different conditions.
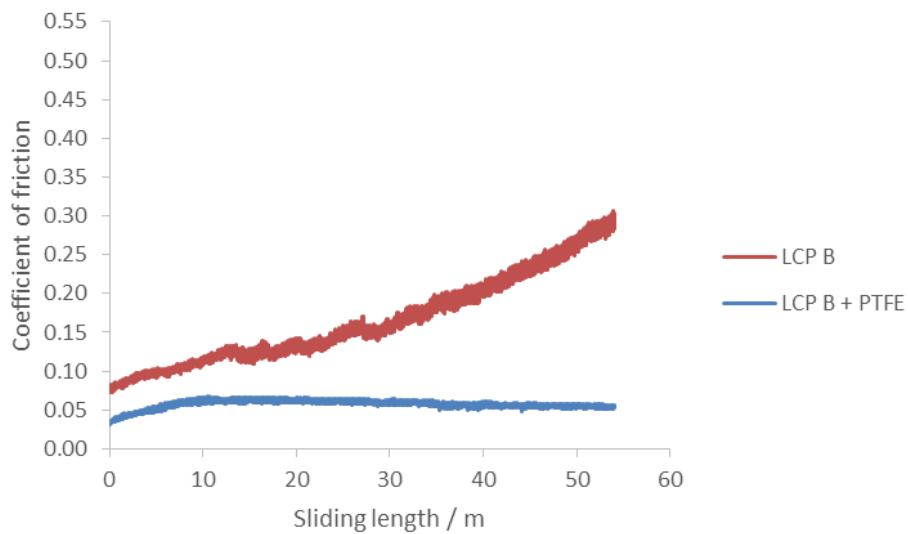

Figure 36 – Comparison of the coefficient of friction between LCP B and LCP B + PTFE coatings for the conditions of 5 N at 5 mm·s^{-1}.

For the load of 10 N, during the test of LCP B coating, the equipment stopped before the total sliding length being completed. This happened since the equipment has a security limit for the value of the coefficient of friction, which was reached.
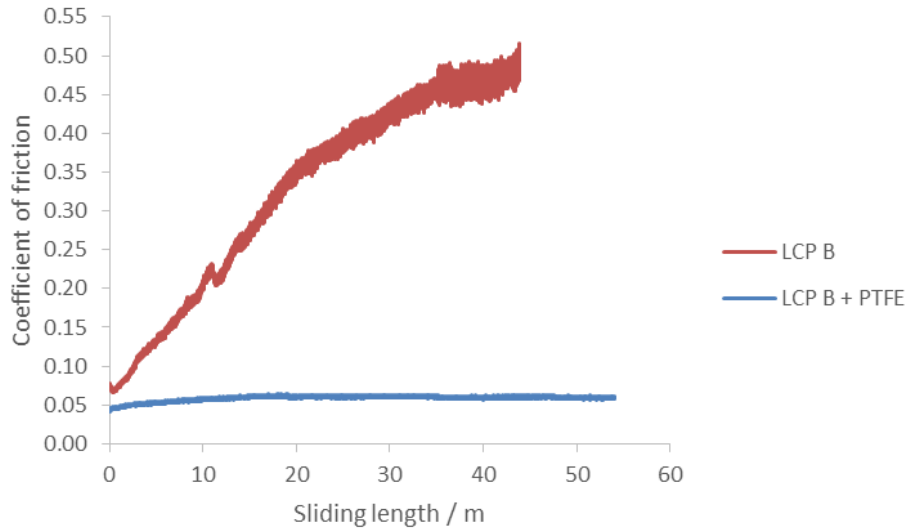
Figure 37 – Comparison of the coefficient of friction between LCP B and LCP B + PTFE coatings for the conditions of 10 N at 10 mm·s^{-1}.

Through the observation of the two previous figures it is possible to see that the coating without PTFE presents a higher coefficient of friction. This occurs due to the absence of the solid lubricant.

As expected, in the coating without PTFE it is observed a rise of the coefficient of friction while in the coating that contains PTFE there is not a significant variation during the test. This phenomenon is explained due to wear debris generation in the coating with PTFE, which form a transfer film of PTFE that acts as a lubricant and which has low coefficient of friction (Myshkin and Goryacheva 2016). The film leads to a contact pair formed by a PTFE counter face and a thin PTFE film (Holmberg and Matthews 2009b).
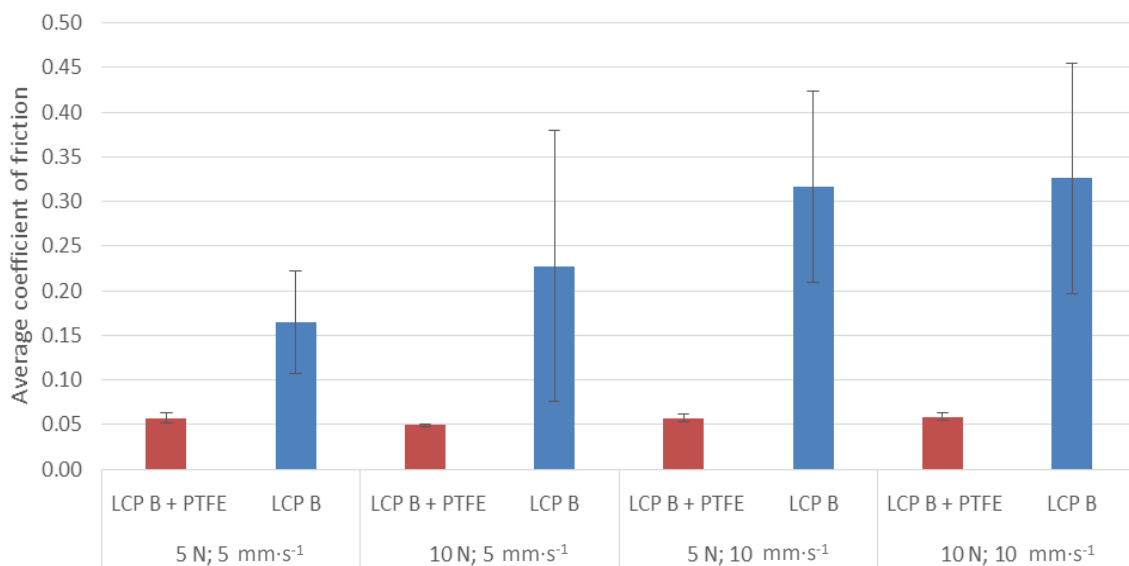

Figure 38 – Average coefficient of friction for the coatings LCP B + PTFE and LCP B, for each condition tested.

Figure 38 shows a comparison of the coefficient of friction for both coatings, with and without PTFE, for each condition tested. Besides the higher values that the coating without PTFE presents, it is also possible to see that the standard-deviation is higher for this coating, as it was expected through the observation of Figure 36 and Figure 37.

4.3.2 Effect of load

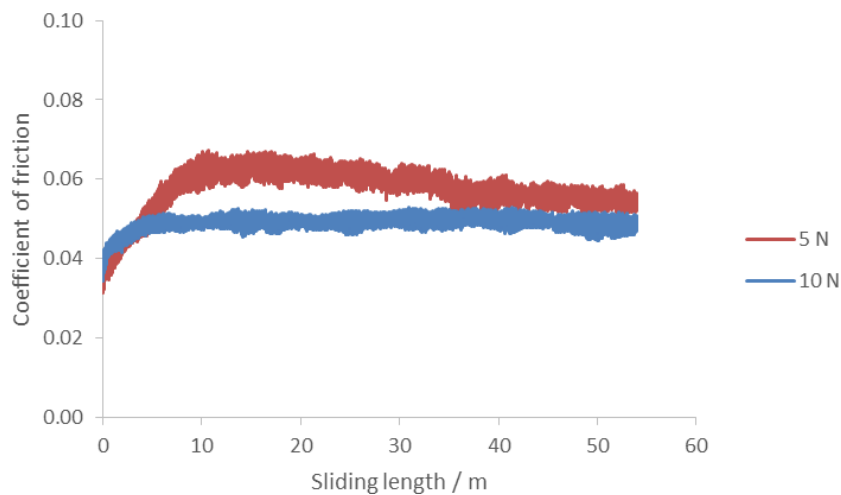Figure 39 and Figure 40 intend to evaluate the effect of the load on the coating containing PTFE.

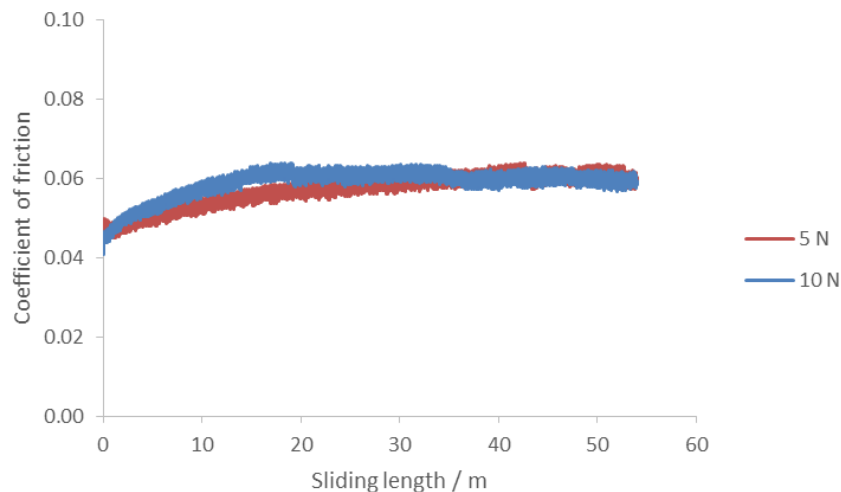*Figure 39 – Coefficient of friction of LCP + PTFE coating for both loads in the condition of 5 mm·s⁻¹.*

Figure 40 - Coefficient of friction of LCP + PTFE coating for both loads in the condition of 10 mm·s⁻¹.

As it was expected, the coefficient of friction remains practically constant since the load applied is in the range 2 N – 100 N (Totten and Liang 2004). As observed, initially there is a rise of the coefficient of friction, followed by stabilization. As the test continues, there is

wear debris generation that attaches by adhesion to the counter face and forms a transfer film. Thus, at a certain time, the contact pair is formed by a PTFE counter face that slides against a thin PTFE film (Holmberg and Matthews 2009b). Since PTFE has very low friction, it helps to control the coefficient of friction and this is the reason why in Figure 39, for the load of 5 N, it is observed an increase and then a decrease of the coefficient of friction before the steady-state is reached.

4.3.3 Effect of sliding velocity

In order to evaluate the effect of the sliding velocity on coating, the load remained constant and the results are presented in Figure 41 and Figure 42.
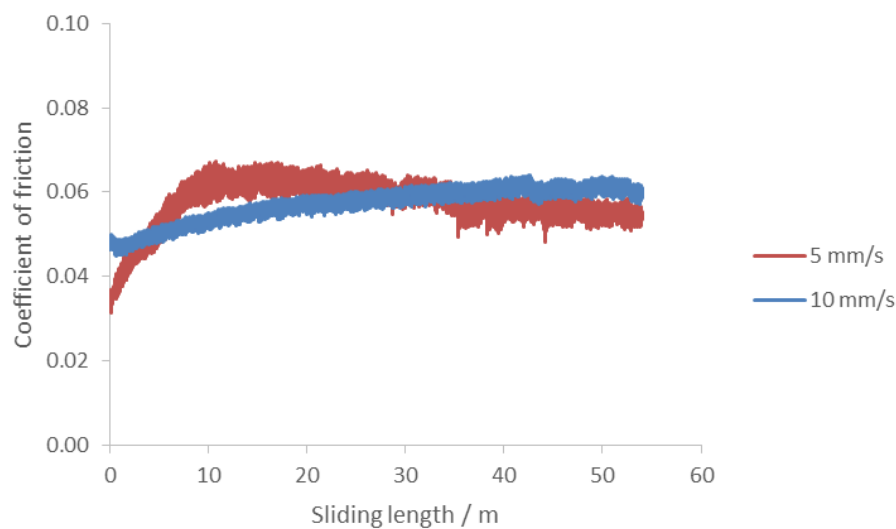

Figure 41 – Coefficient of friction of LCP + PTFE coating for both sliding velocities in the condition of 5 N.
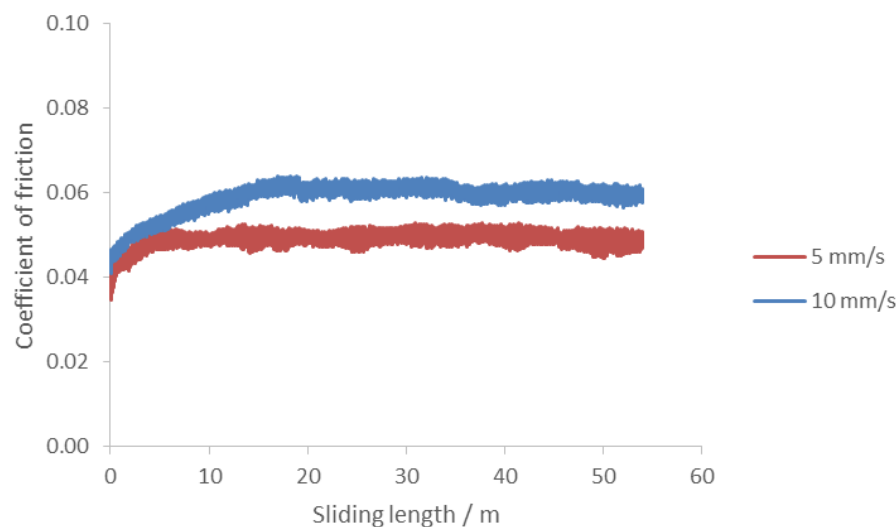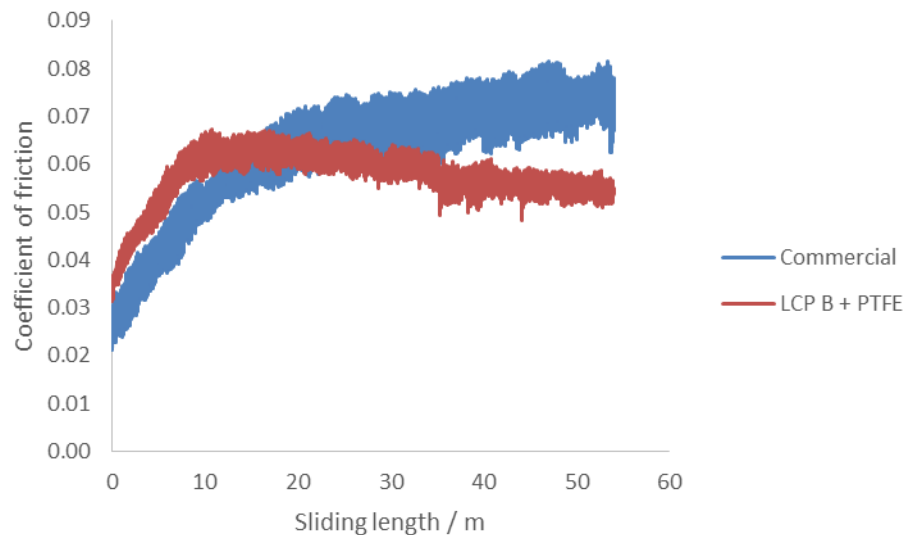

Figure 42 – Coefficient of friction of LCP + PTFE coating for both sliding velocities in the condition of 10 N.

As it can be observed, with the increase of the sliding velocity, the coefficient of friction also increases. This fact might be caused by the rise of the viscous resistance in the contact zone when the contact pressure is high, as it happens in other tribological coatings (Totten and Liang 2004). In Figure 41, initially, for lower sliding velocity there is a rise of the coefficient of friction, which is due to the absence of the film of PTFE explained previously. As it can be seen, the steady-state is reached between 30 m and 40 m of sliding distance, being after this moment that there is confirmed the lower coefficient of friction for a lower sliding velocity.

4.3.4 Comparison with a commercial coating

In order to evaluate the potential of the coating developed, it was compared with a commercial one, being the results presented in Figure 43 and Figure 44. This commercial coating is based on Polyamide-imide (PAI) and contains PTFE as a solid lubricant.

Figure 43 - Comparison of the coefficient of friction between LCP + PTFE and commercial coatings for the conditions of 5 N at 5 mm·s⁻¹.

As it can be observed, there is a situation similar to the one explained previously regarding both LCP B coatings, where it takes a time to stabilise due to the formation of the transfer film. For the conditions of 5 N and 5 mm·s⁻¹, when the steady-state is reached for LCP B + PTFE coating, it is verified that the commercial coating presents a high coefficient of friction. However, it is important to refer that for the commercial coating a steady-state friction level was not verified as this test conditions.
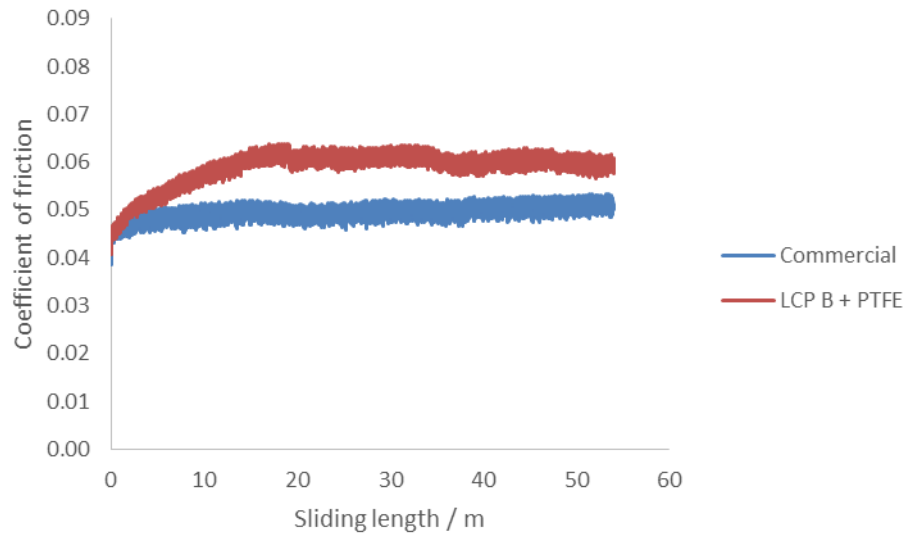
Figure 44 - Comparison of the coefficient of friction between LCP + PTFE and commercial coatings for the conditions of 10 N at 10 mm·s^{-1}.

Regarding the conditions of 10 N and 10 mm·s^{-1}, it is possible to observe that the steady-state is reached sooner for the LCP B + PTFE coating than in the previous conditions and it presents higher coefficient of friction than the commercial coating. Although it can seem that the commercial coating reached the steady-state, it can be observed that the coefficient of friction is increasing. Since the conditions are more aggressive, it leads to the formation of a transfer film sooner, being possible observe a behaviour probably closer to the reality at least for LCP B + PTFE coating. However, the test shall continue to assure the sustainability of the results achieved and verify the steady-state.

Figure 45 shows the comparison of the coefficient of friction for the commercial coating and the LCP B + PTFE, for each condition tested.
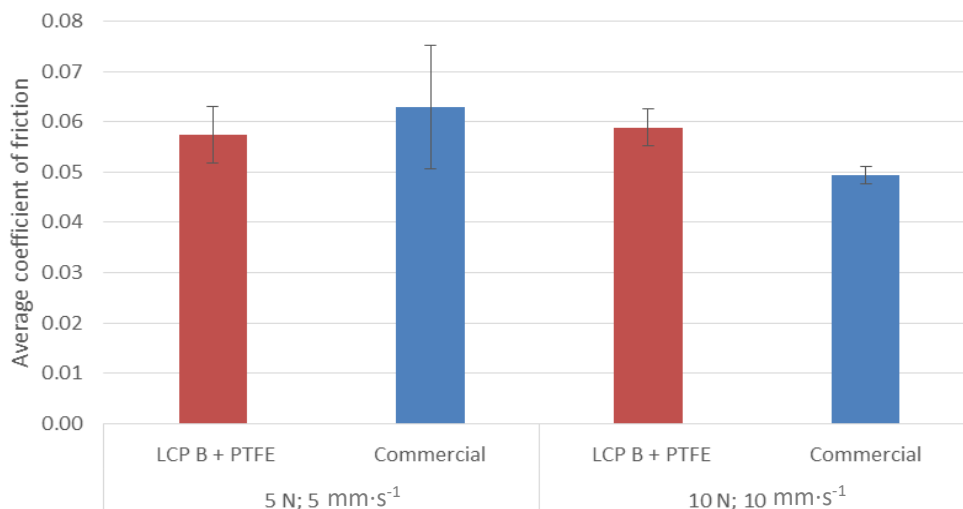

Figure 45 - Average coefficient of friction for the coatings LCP B + PTFE and commercial, for each condition tested.

Through the observation of the previous figure, it is not possible to take conclusions about commercial coating for the conditions of 5 N and 5 mm·s^{-1} since the standard-deviation is too high compared with the other ones. For the conditions of 10 N and 10 mm·s^{-1}, the commercial coating presents a lower coefficient of friction than the LCP B + PTFE coating.

4.3.5 Wear

Figure 46 shows a section of the LCP B coating after the ball on plate test, on top. As it can be observed, there are scratches on the surface that seem to be caused by a ploughing effect and therefore the type of wear might be abrasive. Figure 46 also shows a section of LCP B + PTFE coating after the ball on plate test, below.
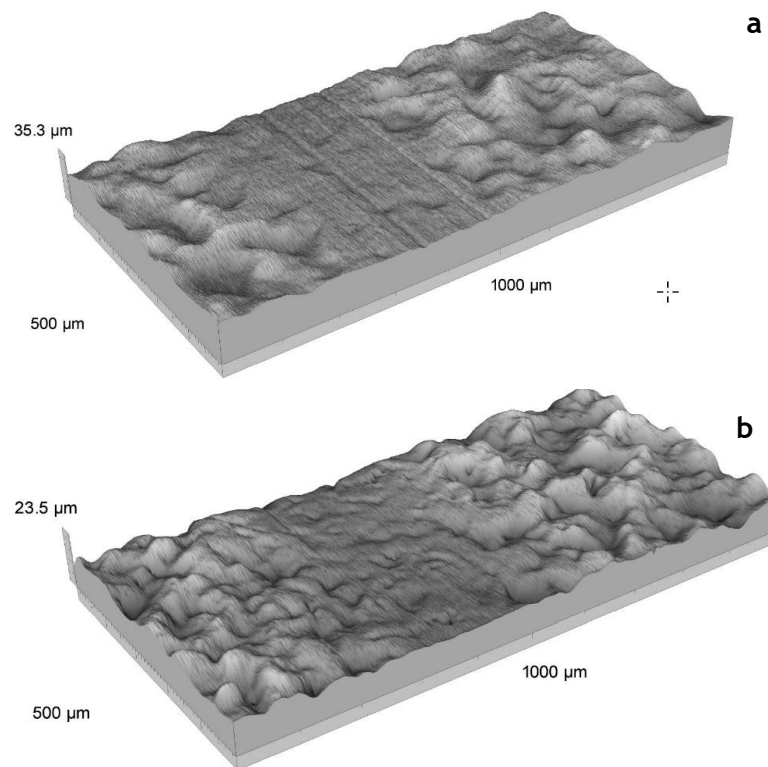
Figure 46 – Examples of worn tracks topography by profilometer.
a) LCP B at 5 N and 10 mm·s^{-1}; b) LCP B + PTFE at 10 N and 10 mm·s^{-1}.

It is presented only one surface topography image of each LCP B coating, as an exemple, since there are tracks where the effect is not visible. In the case of the commercial coating, there is not an image where it is possible to observe the worn track. This is due to the fact that the conditions chosen are too mild for these coatings. Thus, it must be corrected in future work. Figure 47 shows the wear rate and respective standard-deviation for LCP B + PTFE and LCP B coatings.

Figure 47 – Wear rate for the coatings LCP B and LCP B + PTFE, for each condition tested.
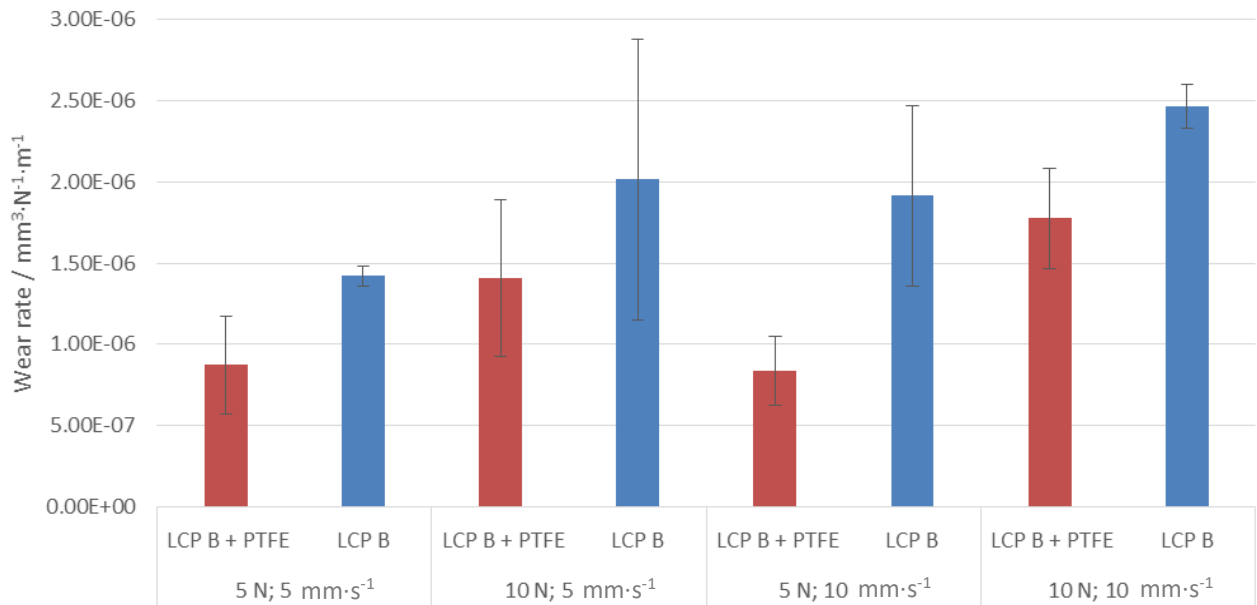
Taking into account the previous figure, it is possible to observe that, in general, the wear rate of the coating containing PTFE is lower than the coating without PTFE. The standard-deviation levels on the measurements are very high and can be due to:

- Some worn tracks are difficult to observe by naked eye and so, in the moment that the profilometer is adjusted to the test, it can be out of the track;
- To get the removed volume calculated by the software, it is necessary to select the area that seems to be worn, which is relative.

Regarding the commercial coating, Figure 48 shows the wear rate of this one and the LCP B + PTFE coating, and their respective standard-deviation.
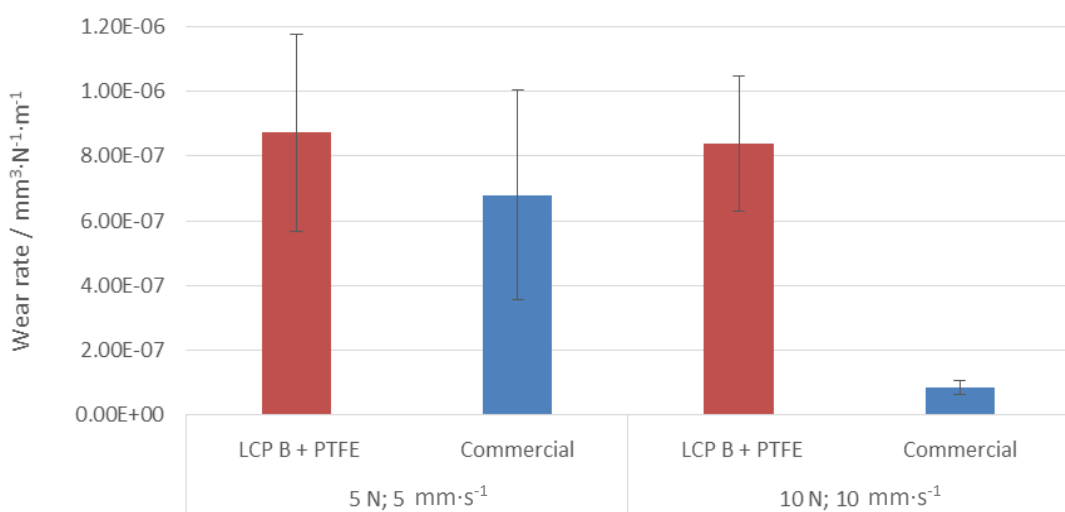

Figure 48 – Wear rate for the coatings LCP B + PTFE and commercial, for each condition tested.

The errors explained before are also applied to the commercial coating, particularly the fact that these tracks are difficult to see by naked eye. Considering these factors and for future work, the best way to solve them would be performed the tribological tests at higher loads in order to allow a more defined worn track.

4.3.5.1   SEM analysis

To observe the worn track topography, it was analysed on SEM. Figure 49 shows the SEM images of the LCP B coating for the conditions of 10 N and 10 mm·s^{-1}.
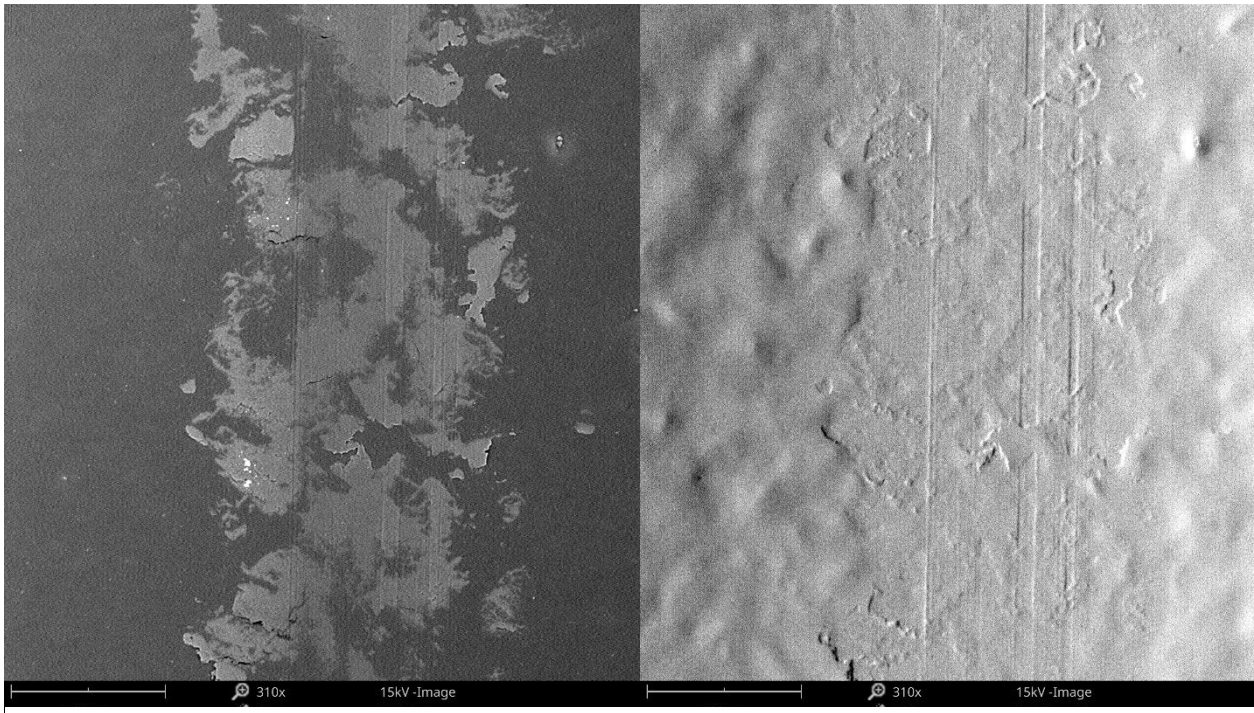
Figure 49 – Worn track of LCP B coating for the conditions of 10 N and 10 mm·s^{-1}.

As it can be seen, there are scratches that seem to be caused by ploughing, as it was already observed in the results given by the profilometer, so the wear might be abrasive.

Figure 50 shows SEM images of the worn track of the LCP B + PTFE coating, for the conditions of 10 N and 10 mm·s^{-1}. As it can be observed, the same scratches are present although they are smoother. The worn track of the coating made on the profilometer does not allow the observation of these scratches, which is consistent with the fact that they are smoother.
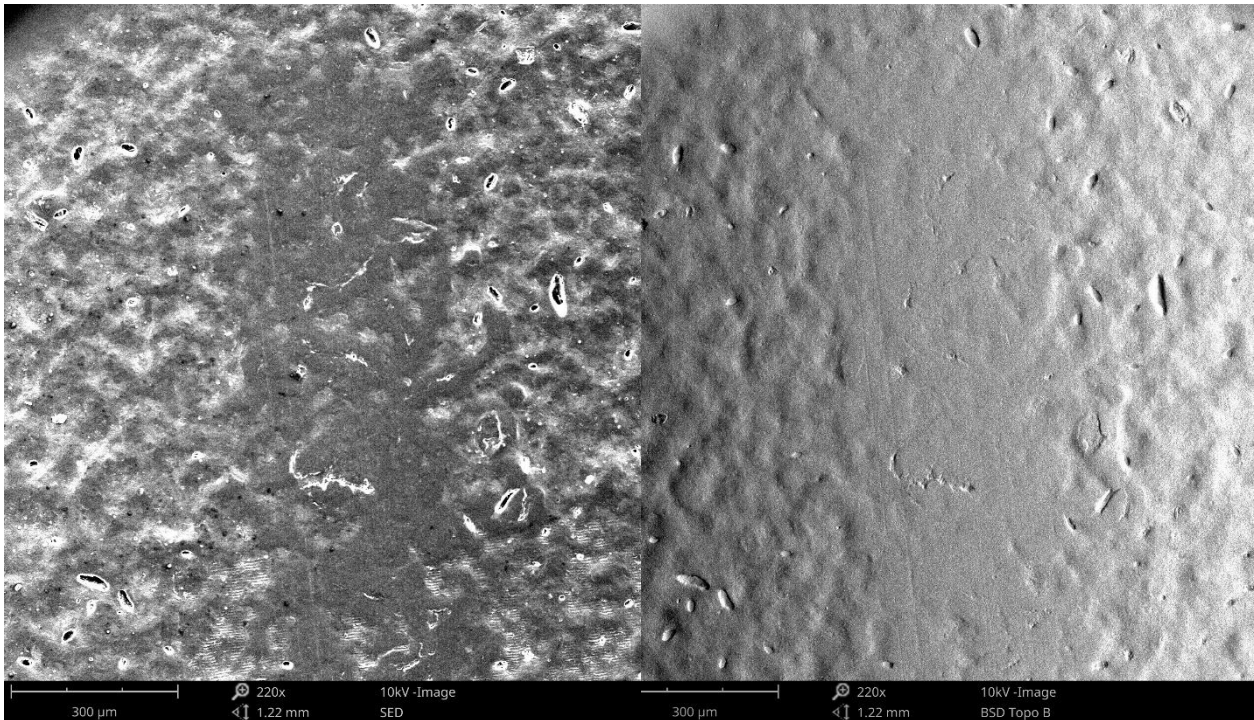
Figure 50 - Worn track of LCP B + PTFE coating for the conditions of 10 N and 10 mm·s⁻¹.

Figure 51 shows the worn track and respective element mapping of the commercial coating, for the conditions of 10 N and 10 mm·s^{-1}.
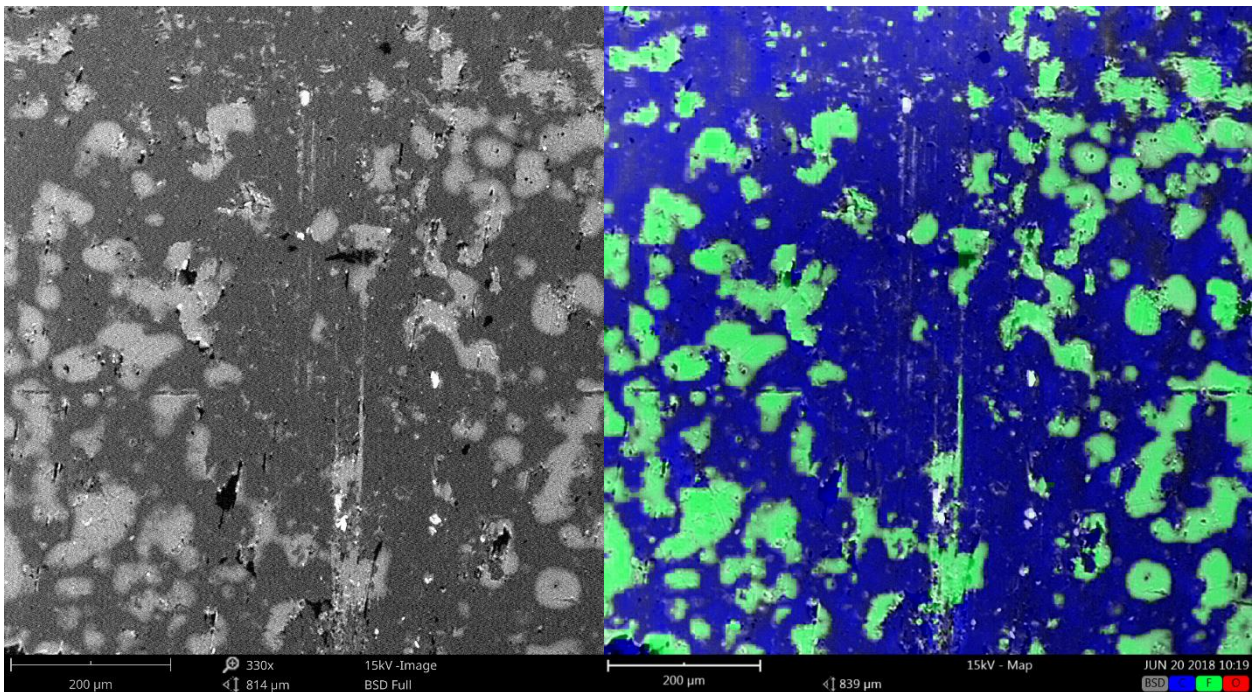
Figure 51 – Worn track of commercial coating for the conditions of 10 N and 10 mm·s⁻¹, at left; element mapping of that coating.

As it can be observed, the worn track is less visible than in the previous coatings, which is consistent with the fact that the image created by the profilometer does not allow to see the track. Through the element mapping it is possible to observe a central zone that contains

less fluorine atoms than the rest, which explains the fact that it was worn since there is less quantity of PTFE.

Figure 52 shows the element mapping of the LCP B coating, at left, and of the LCP B + PTFE coating, at right.
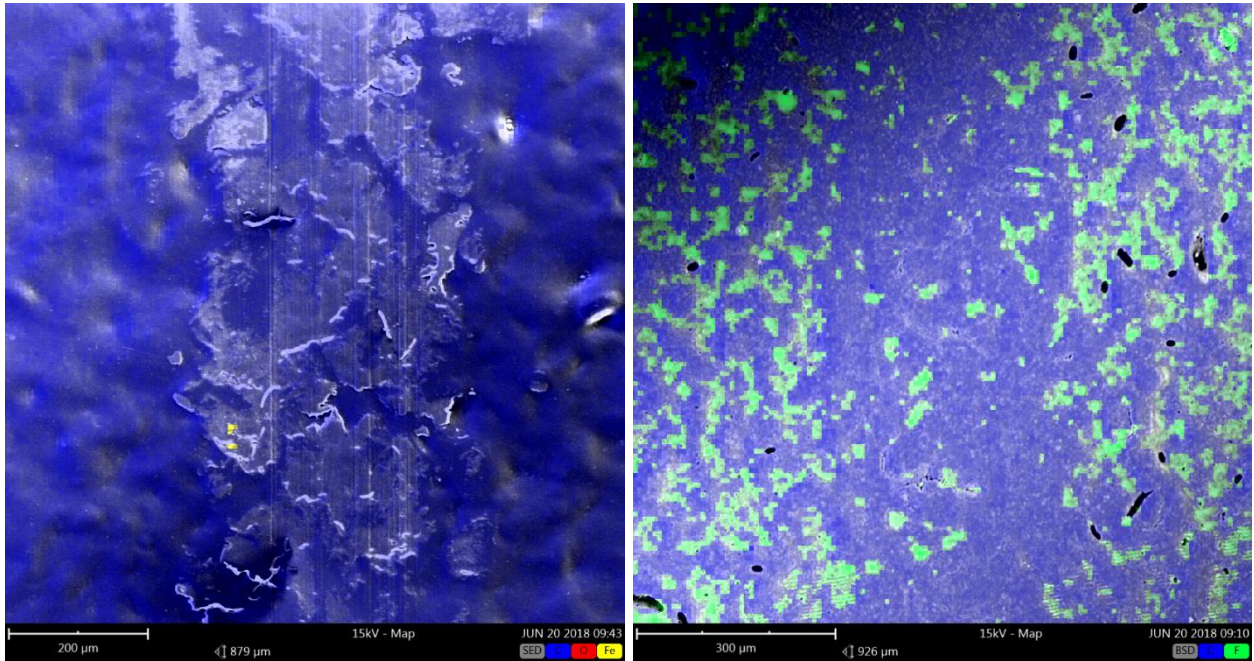
Figure 52 – Element mapping of worn tracks for the conditions of 10 N and 10 mm·s^{-1}. At left, LCP B coating; at right, LCP B + PTFE coating.

Through the previous figure it is possible to observe that for the LCP B coating, there is some Fe, which might be due to:

- The substrate was reached, which is not possible since the wear profiles obtained are not deep enough;
- Some debris removed from the steel ball, which might mean that the coating is so abrasive that can remove steel from the counter face. Since the steel adhered to the coating, the type of wear can therefore be considered adhesive in addition to abrasive.

Regarding the LCP B + PTFE coating, it can be seen that in a central zone there is absence of F and therefore absence of PTFE, which confirms the wearing of the track.

5 Conclusion

The main objective of this project was achieved a coating formulation based on LCP and characterize its tribological properties. From the four types of LCP available, only two of them were soluble. Taking this into account, it was selected LCP B due to an easier use since it is presented as pellet while the LCP A is a powder.

The LCP selected promoted a stable formulation in which it was concluded that the proper solid content is 15 % wt. After the coating application and cure processes, it was observed good adhesion to the substrate, which was crucial to allow continuing to the next phase of the project.

The tribological tests showed a higher coefficient of friction for the coating that does not contain PTFE. The average values of the coefficient of friction are in the range of 0.049 to 0.059 for the coating with PTFE and in the range of 0.227 to 0.326 for the coating that does not contain PTFE. Regarding the effect of the loading, it was observed that the coefficient of friction remains practically constant, as it was expected taking into account the values of load used (5 N and 10 N). Concerning the sliding velocity, it was observed that as far as it increases, the coefficient of friction increases too.

The wear measured did not allow accurate results since the conditions of load and sliding velocity were not intense enough to cause significate effects on the coating.

Concluding, it was achieved a high performance coating that is promising regarding low coefficient of friction that it presents, as it was the objective of the present work. However, the wear has to be measured more rigorously in order to achieve more valid results.

6 Assessment of the work done

6.1 Objectives Achieved

One of the objectives was obtain a stable formulation, which was successfully reached. Besides that, it was possible to formulate a coating based on LCP, which is new in the market for this application and it is promising in terms of tribological properties.

6.2 Limitations and Future Work

One of the objectives was do a physico-chemical characterization of LCP, which was only possible partially. Since it is a commercial product, its chemical structure remains unknown and it was only possible be certainly aware of some linking of LCP. Besides that, some difficulties were presented after checking that the supplier of LCP B closed the Research & Development team that worked in this subject and the product is no longer available. Taking into account that this LCP was the only which reached the solubilization, the suggestions of future work are:

- Try other solvents to solubilize the LCPs that did not achieved a solution.
- Try to solubilize new LCPs since there are a lot of polymers with these characteristics.
- Improve the dispersions that did not work by adjusting or changing the solvent and the additives used.

Regarding wear, the conditions of load and sliding velocity were too low to obtain accurate results, besides the fact that the measurement of wear has associated errors. As far, in the future it can be done:

- Test the tribological performance by using more aggressive conditions, such as higher load and sliding velocity;
- Measure the volume removed from the coating through another equipment that allows more precise results.
- Obtain EDS images of the counter face in order to understand if the Fe present in the coating is from the ball.

6.3 Final Assessment

The main objectives were achieved, with the exception of wear measurement, and, although the limitations already indicated, achieve a product that does not exist in the market

is a gain. The development of this work promoted critical sense and a deeper knowledge about the cycle of creation of a product in this field as well as about tribology and the concepts surrounding it.

The project developed allows the company to continue it in the future since there are basis with potential to improve the work already done and to can achieve a product that can be sold in the coating market.

References

- "Azonano". Accessed 24/06/2018. https://www.azonano.com/article.aspx?ArticleID=4708.

- Báron, M. Definitions of basic terms relating to low-molar-mass and polymer liquid crystals (IUPAC Recommendations 2001). *Pure Appl. Chem.* no. **73**, 845-895. 2001.

- Bhushan, B. Friction. In *Introduction to Tribology*, John Wiley & Sons, 2nd ed., Vol. **56**, 2013a.

- Bhushan, B. Introduction. In *Introduction to Tribology*, John Wiley & Sons, 2nd ed., Vol. **56**, 2013b.

- Bhushan, B. Introduction. In *Principles and applications of tribology*, John Wiley & Sons, 2nd ed., Vol. **56**, 2013c.

- Bhushan, B. Wear. In *Introduction to Tribology*, John Wiley & Sons, 2nd ed., Vol. **56**, 2013d.

- Brostow, W., Deborde J.-L., Jaklewicz M. and Olszynski P. Tribology with emphasis on polymers: Friction, scratch resistance and wear. *Journal of Materials Education* no. **24**, 119-132. 2003.

- "Bruker". Accessed 25/05/2018. https://www.bruker.com/products/surface-and-dimensional-analysis/tribometers-and-mechanical-testers/umt-tribolab/overview.html.

- Carrión, F.-J., Martínez-Nicolás G., Iglesias P., Sanes J. and Bermúdez M.-D. Liquid Crystals in Tribology. *International Journal of Molecular Sciences* no. **10** (9), 4102-4115. 2009.

- Cosimo, C., Marta G. and Eugenio A. Can liquid crystalline polymers find application in the field of protective coatings? *Anti-Corrosion Methods and Materials* no. **46** (2), 95-99. 1999.

- Das, T., Banthia A. K., Adhikari B. and Alam S. Binary Blends of Polytetrafluoroethylene and Liquid Crystalline Polymer. *Polymer-Plastics Technology and Engineering* no. **45** (9), 1047-1052. 2006.

- E. Banks, R., E. Smart B. and C. Tatlow J. Fluoropolymer coatings. In *Organofluorine Chemistry: Principles and Commercial Applications*, 1994.

- "GGB". Accessed 29/03/2018. https://www.ggbearings.com/en/company/tribology.

- Holmberg, K. and Matthews A. Applications. In *Coatings tribology: properties, mechanisms, techniques and applications in surface engineering*, Elsevier Science, 2009a.

- Holmberg, K. and Matthews A. Tribology of coatings. In *Coatings tribology: properties, mechanisms, techniques and applications in surface engineering*, Elsevier Science, 2009b.

- Hutchings, I. M. Leonardo da Vinci's studies of friction. *Wear* no. **360-361**, 51-66. 2016.

- Jin, Z. M., Zheng J., Li W. and Zhou Z. R. Tribology of medical devices. *Biosurface and Biotribology* no. **2** (4), 173-192. 2016.

- "Laboratory-Equipment". Accessed 03/04/2018. https://www.laboratory-equipment.com/dispersers/t-25-digital-ultra-turrax-disperser-ika.php.

- Lebedev, Y. A., Korolev Y. M., Polikarpov V. M., Ignat'eva L. N. and Antipov E. M. X-ray powder diffraction study of polytetrafluoroethylene. *Crystallography Reports* no. **55** (4), 609-614. 2010.

- McKeen, L. W. Additives. In *Fluorinated Coatings and Finishes Handbook*, William Andrew Publishing, 2006a.

□ McKeen, L. W. Application of Liquid Coatings. In *Fluorinated Coatings and Finishes Handbook*, William Andrew Publishing, 2006b.

□ McKeen, L. W. Binders. In *Fluorinated Coatings and Finishes Handbook*, William Andrew Publishing, 2006c.

□ McKeen, L. W. Pigments, Fillers and Extenders. In *Fluorinated Coatings and Finishes Handbook*, William Andrew Publishing, 2006d.

□ McKeen, L. W. Producing Monomers, Polymers and Fluoropolymer Finishing. In *Fluorinated Coatings and Finishes Handbook*, William Andrew Publishing, 2006e.

□ McKeen, L. W. Solvent Systems. In *Fluorinated Coatings and Finishes Handbook*, William Andrew Publishing, 2006f.

□ McKeen, L. W. Substrates and Substrate Preparation. In *Fluorinated Coatings and Finishes Handbook*, William Andrew Publishing, 2006g.

□ Miyauchi, K., Watanabe H. and Yuasa M. A study of adhesive improvement of a Cr-Ni alloy layer on a liquid crystal polymer (LCP) surface. *Progress in Organic Coatings* no. **94**, 73-78. 2016.

□ Müller, B. and Poth U. Pigment dispersions. In *Coatings Formulation: An International Textbook*, Vincentz Network GmbH & Co. KG, Second ed., 2011.

□ Myshkin, N. K. and Goryacheva I. G. Tribology: Trends in the half-century development. *Journal of Friction and Wear* no. **37** (6), 513-516. 2016.

□ P. Jose, J. and Joseph K. Kevlar Fiber-Reinforced Polymer Composites. In *Advances in Polymer Composites: Macro- and Microcomposites*, p. 1-16, 2012.

□ Pavel, D., Hibbs D. and Shanks R. Review of main chain liquid crystalline polymers. *Advanced Research in Polymer Science*, 65-84. 2006.

□ Roberts, E. W. Space tribology: its role in spacecraft mechanisms. *Journal of Physics D: Applied Physics* no. **45** (50). 2012.

□ Shibaev, V. Liquid Crystalline Polymers. In *Reference Module in Materials Science and Materials Engineering*, Elsevier, p. 1-46, 2016.

□ Theo, M. Lubricants and Lubrication. In *Ullmann's Encyclopedia of Industrial Chemistry*, Vol. **1-39**, p. 6-11, 2011.

□ Totten, G. E. and Liang H. Mechanical Behavior of Plastics: Surface Properties and Tribology. In *Mechanical tribology: materials, characterization, and applications*, Marcel Dekker, 2004.

□ W. Robinson, J., Zhou Y., Bhattacharya P., Erck R., Qu J., Timothy Bays J. and Cosimbescu L. Probing the molecular design of hyper-branched aryl polyesters towards lubricant applications. *Scientific reports* no. **6**, 18624. 2016.

□ Wang, X. J. and Zhou Q. F. Liquid Crystalline Polymers as High Performance Fiber and Structural Materials. In *Liquid Crystalline Polymers*, World Scientific, 2004.

□ "Wayne State University". 2008. Accessed 28/03/2018. http://www.physics.wayne.edu/~glawes/lc.pdf.

□ Wen, S. and Huang P. Properties of Lubricants. In *Principles of Tribology*, John Wiley & Sons, p. 1-455, 2012.

□ Xuefeng, W., Jonathan E. and Chang L. Liquid crystal polymer (LCP) for MEMS: processes and applications. *Journal of Micromechanics and Microengineering* no. **13** (5), 628-633. 2003.

▫ Yamamoto T, B., D.H. Wear Mechanism Based on Adhesion. *NASA Thechnical Paper 2037*. 1982.